

Out-of-time-order correlator, many-body quantum chaos, light-like generators, and singular values

Ke Huang,¹ Xiao Li,^{1,*} David A. Huse,² and Amos Chan^{3,†}

¹*Department of Physics, City University of Hong Kong, Kowloon, Hong Kong SAR, China*

²*Department of Physics, Princeton University, Princeton, New Jersey 08544, USA*

³*Physics Department, Lancaster University, Lancaster, LA1 4YW, United Kingdom*

(Dated: October 10, 2023)

We study out-of-time-order correlators (OTOCs) of local operators in spatial-temporal invariant or random quantum circuits using light-like generators (LLG) — many-body operators that exist in and act along the light-like directions. We demonstrate that the OTOC can be approximated by the leading singular value of the LLG, which, for the case of generic many-body chaotic circuits, is increasingly accurate as the size of the LLG, w , increases. We analytically show that the OTOC has a decay with a universal form in the light-like direction near the causal light cone, as dictated by the sub-leading eigenvalues of LLG, z_2 , and their degeneracies. Further, we analytically derive and numerically verify that the sub-leading eigenvalues of LLG of any size can be accessibly extracted from those of LLG of the smallest size, i.e., $z_2(w) = z_2(w = 1)$. Using symmetries and recursive structures of LLG, we propose two conjectures on the universal aspects of generic many-body quantum chaotic circuits, one on the algebraic degeneracy of eigenvalues of LLG, and another on the geometric degeneracy of the sub-leading eigenvalues of LLG. As corollaries of the conjectures, we analytically derive the asymptotic form of the leading singular state, which in turn allows us to postulate and efficiently compute a product-state variational ansatz away from the asymptotic limit. We numerically test the claims with four generic circuit models of many-body quantum chaos, and contrast these statements against the cases of a dual unitary system and an integrable system.

Introduction.— A generic interacting quantum many-body system obeys the eigenstate thermalization hypothesis (ETH) and evolves towards the local equilibrium state [1–3]. During this process, information of local perturbation spreads among non-local degrees of freedom of the system, and can be diagnosed using the out-of-time-order correlator (OTOC) [4–6], a correlation function between multiple operators probed at times which are out of order [7–29]. Recent developments of random quantum circuits as toy models of spatially-extended many-body quantum chaotic systems have led to discoveries of a plethora of novel phenomena [30–48]. In particular, the Floquet operator of a given generic quantum many-body circuit, a *space-like generator*, captures novel signatures in spectral correlation [36, 49–52] and eigenstate correlation [53, 54] beyond those described in the random matrix theory and ETH; while its associated space-time dual transfer matrix, a *time-like generator*, have been found to exhibit non-unitary dynamics [36, 37, 39, 55–61], and remarkably belongs to the universality class of the Ginibre ensemble [62, 63]. *Light-like generators* (LLGs) [41, 64–68] are many-body operators that exist in and act along the LL directions [Fig. 1(d-e)]. There are at least two reasons why the study of LLGs is interesting. Firstly, correlation functions of local operators, e.g., two-point correlation function and OTOC, in quantum circuits can naturally be written in terms of LLGs due to the upper bound on the propagation speed of quantum information as given by the causal light cone. Secondly, as we will argue and demonstrate below, LLG captures universal signatures of many-body quantum dynamics. As a heuristic, along

the LL direction, OTOC can be generated from a LLG of a fixed length, and takes the values around 0, 1, and 0 sequentially, exhibiting the “010”-behavior for generic chaotic circuits [Fig. 1(a)]. Such phenomena suggest that the full behavior of OTOC cannot be dictated by the leading eigenvalues of LLGs, and in fact, the non-normal nature of LLGs underlies the universal features of OTOC.

Models.— We consider many-body quantum systems modelled by unitary circuits of two-site gates arranged in the brick-wall geometry, $U(t) = \prod_{s=1}^t \bigotimes_{i \in 2\mathbb{Z} + s \bmod 2} u_{i,i+1}$, where $u_{i,i+1}$ are q^2 -by- q^2 unitary operator acting on site i and $i + 1$, see Fig. 1. These two-site gates are selected to model three different dynamics without local conserved quantities, including: (i) four models displaying generic many-body quantum chaos, namely the Haar-random (HRM), random phase (RPM), three-parameter (3PM) models, and a variant of HRM with Z_2 and time-reversal symmetry (Z_2 -COE) [to compare with (iii) below]; (ii) a DU model, and (iii) an integrable model called the XYZ circuit (XYZc). The precise definitions of these models are provided in supplementary material (SM) [69] and are not important to the derivations of results below. We study mainly two symmetry classes, namely the spatial-temporal invariant circuits whose gates are all identical, and the spatial-temporal random circuits whose gates are independently chosen from certain ensemble. Ensemble averages are taken for the spatial-temporal random circuits but not for the invariant ones.

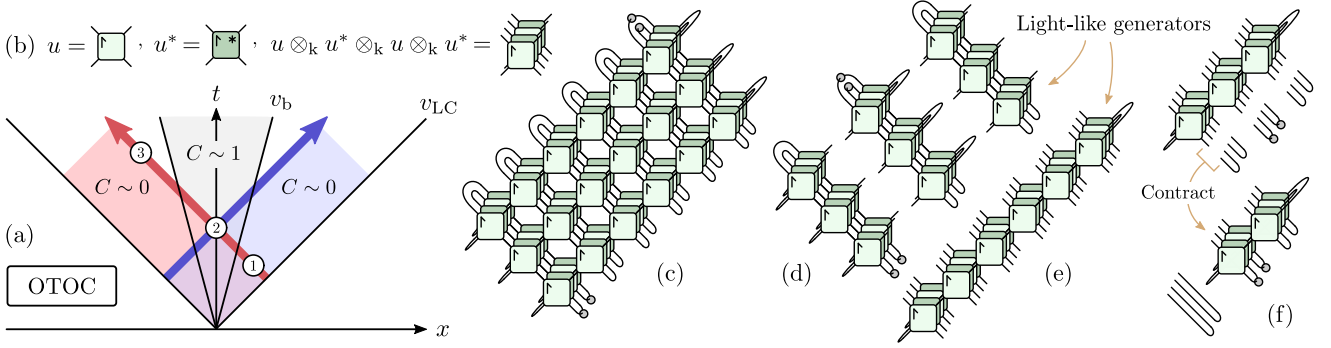


FIG. 1. (a) Illustration of the behaviour OTOC $\tilde{C}(x, t) = C(w, \tau)$ in the x and t plane (or w and τ plane). $C \sim 1$ sufficiently within region 2, the butterfly cone, defined by the butterfly velocity v_b [31, 32], in which the operator spreads. $C \sim 0$ in regions 1 and 3 outside the above region but inside the system’s causal light cone defined by the light cone velocity v_{LC} . The LLG can be used to generate OTOC along the red arrow, which goes through the regime $C \sim 0$, $C \sim 1$ and $C \sim 0$ in sequence, the “010-behavior”, implying non-trivial properties of the generators. (b) The diagrammatical representation of unitary gates and their conjugates. (c) The representation of OTOC $\tilde{C}(x = 2, t = 8) = C(w = 6, \tau = 3)$ after the annihilation of unitaries and their conjugates outside the light cone. The grey circles represent the (generalization of) Pauli operators. The OTOC can be generated by (d) $(\tilde{L}_\tau, |\tilde{R}_\tau)$, and the right-moving LLG; or the (e) left-moving many-body LLG. (f) LLG of size w can be reduced to LLG of size $w' < w$ upon contraction with certain states.

Light-like generators.— The OTOC is defined as

$$\begin{aligned} \tilde{C}(x, t) &:= \frac{1}{2} \langle [\sigma(0, t), \sigma(x, 0)]^\dagger [\sigma(0, t), \sigma(x, 0)] \rangle \\ &= 1 - \langle \sigma(0, t) \sigma(x, 0) \sigma(0, t) \sigma(x, 0) \rangle, \end{aligned} \quad (1)$$

where $\sigma(x, t) = U(t) \sigma_x [U(t)]^\dagger$, and σ_x is a hermitian and unitary local operator acting on site x . To represent OTOC, it is convenient to define a tensor product of unitary gates in the replicated space with $\mathcal{U}_2 \equiv u \otimes_k u^* \otimes_k u \otimes_k u^*$ [Fig. 1(b)] and states in the replicated space with

$$|0_{\sigma, \mu}\rangle := \frac{1}{\sqrt{q}} \begin{array}{c} \textcircled{\sigma} \\ \textcircled{\mu} \end{array}, \quad |1_{\sigma, \mu}\rangle := \frac{1}{\sqrt{q}} \begin{array}{c} \textcircled{\sigma} \\ \textcircled{\mu} \end{array}, \quad (2)$$

where σ, μ are identities or the (generalization of) Pauli matrices. We further define $|0\rangle \equiv |0_{1,1}\rangle$ and $|1\rangle \equiv |1_{1,1}\rangle$. By annihilating pairs of unitary gates and their conjugates outside of the light cone, as illustrated in Fig. 1(c), the OTOC can also be expressed in terms of LLGs,

$$\begin{aligned} C(w, \tau) &:= \tilde{C}(x = w - \tau - 1, t = w + \tau - 1) \\ &= 1 - \langle L_w | T_{L,w}^\tau | R_w \rangle = 1 - \langle \tilde{L}_\tau | T_{R,\tau}^{w-2} | \tilde{R}_\tau \rangle, \end{aligned} \quad (3)$$

where $w = (t + x)/2 + 1$ and $\tau = (t - x)/2$ are the shifted light cone coordinate labelling the diagonal width and length of the overlapped light cone region of the two local operators in the OTOC [see Fig. 1(c)]. The left-moving and right-moving LLGs are, $T_{L,w} = \langle 0 | \textcircled{\sigma}_r^w \mathcal{U}_2 | 1 \rangle$ and $T_{R,w} = \langle 1 | \textcircled{\sigma}_l^w \mathcal{U}_2 | 0 \rangle$, as illustrated in Fig. 1(e) and 1(d). $\textcircled{\sigma}_r$ ($\textcircled{\sigma}_l$) denotes the contraction between the northeast (northwest) legs of a tensor with the southwest (southeast) leg of another tensor.

Similarly, angle (round) brackets denote vectors with open legs along the left-going (right-going) LL direction. The initial and final states associated with the left-going LLG are given by $\langle L_w | = \langle 1^{w-1} | \otimes \langle 1_{\sigma, \sigma} |$, and $|R_w\rangle = |0_{\sigma, \sigma}\rangle \otimes |0^{w-1}\rangle$, where we have defined $\langle 1^w | := \bigotimes_r^w \langle 1 |$ and similarly for the other states. The initial and final states associated with the right-going LLG are $\langle \tilde{L}_w | = \langle 0^w | [\langle 1 | \textcircled{\sigma}_l^w \mathcal{U}_2 | 0_{\sigma, \sigma} \rangle]$, and $|\tilde{R}_w\rangle = [\langle 1_{\sigma, \sigma} | \textcircled{\sigma}_l^w \mathcal{U}_2 | 0 \rangle] |1^w\rangle$. For succinctness, the subscript R, L of the LLG will be hidden if the discussion applies to both directions. One can prove that the moduli of all eigenvalues of T_w are equal or less than 1 [69]. An obvious pair of left and right eigenstates of T_w with eigenvalue 1 is $\langle 1^w |, |0^w\rangle$, normalized such that $\langle 1^w | 0^w \rangle = 1$. Generally, we find that these are the only eigenstates with eigenvalue 1 except for the DU case, i.e., the subleading eigenvalue of T_w satisfies $|z_2(w)| < 1$. Hence, if we remove the leading eigenvalue from T_w and define $F_w := T_w - |0^w\rangle\langle 1^w|$, we can write

$$C(w, \tau) = - \langle L_w | F_{L,w}^\tau | R_w \rangle = - \langle \tilde{L}_\tau | F_{R,\tau}^{w-2} | \tilde{R}_\tau \rangle. \quad (4)$$

Here, we have used $F_w^\tau = T_w^\tau - |0^w\rangle\langle 1^w|$ and $\langle L_w | 0^w \rangle = \langle 1^w | R_w \rangle = 1$.

F_w and T_w are both nonnormal matrices, so their operator norms are not solely determined by their eigenvalues. It turns out that their operator norms satisfy [69]

$$\lim_{w \rightarrow \infty} \|T_w\| = q^\alpha, \quad \lim_{w \rightarrow \infty} \frac{\|F_w\|}{q^w} = 1, \quad (5)$$

where $0 \leq \alpha \leq 1$ is independent of w . The second relation is a direct result of the w -independence of α , because $F_w = -|0^w\rangle\langle 1^w| + T_w$ and the first

TABLE I. Summary of properties of the LLGs of generic quantum many-body chaotic circuits, and DU circuits.

	Generic Chaos	Dual Unitary
Block Structure	Upper-triangular	Diagonal
Lead. sing. val. of T_w^τ	q^w ($\tau \gg w$) q^α ($\tau = 1, w \gg 1$)	1
Lead. eig. val. of F_w	$z_2(w) = z_2(w=1) < 1$ $a(z_2) \stackrel{\text{conj}}{=} w$ $g(z_2) \stackrel{\text{conj}}{=} 1$	$z_2(w) = 1$ $a(z_2) \geq w$ $g(z_2) = a(z_2)$
Lead. sing. val. of F_w^τ	$\tau^{w-1} z_2^\tau$ ($\tau \gg w$) q^w ($\tau \lesssim w, w \gg 1$)	q^w
Lead. sing. state of F_w^τ	$ 1^{w-1}\rangle \otimes z_2\rangle$ ($\tau \gg w$) $ 1^w\rangle$ ($\tau \lesssim w, w \gg 1$)	Exactly solvable & τ -independent

term dominates the operator norm. If the subleading eigenvalue $z_2(w)$ of T_w is less than 1, the large- τ behavior of the LLG is described by [69]

$$\lim_{\tau \rightarrow \infty} \|F_w^\tau\| = 0, \quad \lim_{\tau \rightarrow \infty} \|T_w^\tau\| = q^w. \quad (6)$$

Moreover, as $\|F_w^\tau\|$ is still dominated by $|0^w\rangle\langle 1^w|$ for $\tau < w/\alpha$, there is a plateau at $\|F_w^\tau\| \approx q^w$ before the inevitable decay, which differentiates F_w from the normal matrices. The asymptotic behaviors of LLG for the cases of generic chaos and DU (discussed below) are summarized in Table. I.

Recursivity and symmetries.— For systems with translation symmetries in space and in time, the LLG of a given size can be reduced to smaller ones,

$$F_w |0^m\rangle \otimes |\psi\rangle = |0^m\rangle \otimes (F_{w-m} |\psi\rangle), \quad (7)$$

$$\langle \psi | \otimes \langle 1^m | F_w = (\langle \psi | F_{w-m}) \otimes \langle 1^m |,$$

where $|\psi\rangle$ is an arbitrary state. Hence, we can decompose the Hilbert space into four orthogonal subspaces, $P_{0\bar{1}}, P_{0\bar{1}}, P_{01}, P_{0\bar{1}}$ where the subscript 0 and 1 denote the states with $|0\rangle$ on the leftmost site of the LLG and $|1\rangle$ on the rightmost one, and the bar denotes that the state on the leftmost (rightmost) site is orthogonal to $|0\rangle$ ($|1\rangle$). Note that the irreducible subspace is $P_{01} + P_{0\bar{1}}$ for the ket states, and $P_{0\bar{1}} + P_{0\bar{1}}$ for the bra states. In terms of these four sectors, the LLG for $w \geq 2$ becomes block-upper-triangular, schematically illustrated by

$$F_w = \begin{bmatrix} 0\bar{1} & \bar{0}\bar{1} & 01 & \bar{0}1 \\ \tilde{F}_{w-1}^{(11)} & \tilde{F}_w^{(12)} & \tilde{F}_{w-1}^{(13)} & \tilde{F}_w^{(14)} \\ 0 & \tilde{F}_w^{(22)} & 0 & \tilde{F}_w^{(24)} \\ 0 & 0 & \tilde{F}_{w-2}^{(33)} & \tilde{F}_{w-1}^{(34)} \\ 0 & 0 & 0 & \tilde{F}_{w-1}^{(44)} \end{bmatrix}, \quad (8)$$

where $\tilde{F}_w^{(ij)}$ is a tensor obtained from contracting a LLG of size w , and the superscripts of $\tilde{F}_w^{(ij)}$ denote the position of the block in the matrix. In particular, we have $\tilde{F}_{w=0}^{(33)} = 0$. Hence, the eigenvalues of F_w are determined by the

diagonal blocks. We can further show that the blocks in red and blue separately constitute a LLG of width $w-1$, that $\tilde{F}_{w-2}^{(33)}$ is identical to F_{w-2} , and that $\tilde{F}_w^{(22)}$ in green is a block that appears in F_w , but not in smaller LLG [69]. Consequently, we can obtain recursively for $w \geq 2$ that

$$a(z, w) = 2a(z, w-1) - a(z, w-2) + \tilde{a}(z, w), \quad (9)$$

where $a(z, w)$ and $\tilde{a}(z, w)$ are respectively the algebraic multiplicity of each eigenvalue z of F_w and $\tilde{F}_w^{(22)}$. In particular, when z is not an eigenvalue of F_w ($\tilde{F}_w^{(22)}$), we set $a(z, w) = 0$ ($\tilde{a}(z, w) = 0$). We further define $a(z, w = 0) \equiv 0$. Among these eigenvalues, the leading eigenvalue $z_2(w)$ of F_w is particularly important, as it partially determines the decay rate along the LL direction (see Eq. (13) below). Under mild assumptions, one can prove that the asymptotic decay rate of $C(w, \tau)$ is limited by the decay rate of $F_{w=1}$, i.e., all eigenvalues z of F_w satisfy $|z| \leq |z_2(w=1)|$, and hence there always exists [69]

$$z_2(w) = z_2(w=1), \quad (10)$$

regardless of whether the system is integrable or chaotic. In other words, $z_2(w)$, and hence the OTOC decay rate Eq. (13), are generally accessible through LLG of width $w=1$. Furthermore, we observe that the LLG generically has only one leading eigenvalue, and therefore $a(z_2, w=1) = 1$. These statements are rigorously proved for the ensemble-averaged LLG for the spatial-temporal random HRM [69]. If the system is chaotic, it is natural to assume that the eigenvalues of the new block $\tilde{F}_w^{(22)}$ are not fine-tuned, i.e., they are not identical to those of any smaller LLGs. Hence, we have **Conjecture 1 on circuit models of generic many-body quantum chaos**: if z is an eigenvalue of F_{w-1} , then

$$\tilde{a}(z, w) = 0. \quad (11)$$

Particularly, we have $\tilde{a}[z_2(w), w] = 0$. Furthermore, the geometric multiplicity $g[z_2(w), w]$ generally does not increase and remains to be 1 because the off-diagonal blocks are not expected to be zero for generic chaotic models. Hence, we introduce **Conjecture 2 on circuit models of generic many-body quantum chaos**:

$$g[z_2(w), w] = 1. \quad (12)$$

Consequently, the LLG is not only non-normal, but generally non-diagonalizable. This reducibility also suggests that the OTOC is described by some smaller LLGs F_{w-m} if one of the initial states is reducible, while only the OTOC with irreducible initial states, such as $\langle L_w |, |R_w \rangle$, is truly governed by F_w . Note that $(\tilde{L}_w |, |\tilde{R}_w \rangle)$ contain both irreducible and reducible components which are controlled by LLGs of different sizes.

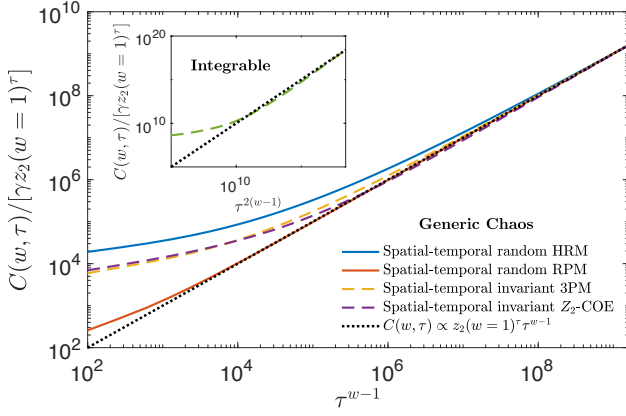


FIG. 2. Verifications of Eq. (10) and Conjectures 1 and 2. The large τ behavior of the OTOC for four generic chaotic circuit models. The inset shows an integrable model, the XYZc model, with a distinct scaling behavior. Here, we take $w = 5$, and γ is a non-universal model-dependent constant derived from fitting.

Large τ behavior.— In the large τ limit, the OTOC eventually decays according to [69],

$$C(w, \tau) \propto \lambda_{w, \tau} \propto \tau^{\varphi[z_2(w), w]} z_2(w)^\tau, \quad (13)$$

where $\varphi(z, w) = N_{\max}(z, w) - 1$, and $N_{\max}(z, w)$ is the dimension of the largest Jordan block corresponding to eigenvalue z . From the two conjectures, and the empirical result $a(z_2, w = 1) = 1$, we have, for generic chaotic circuit models,

$$\varphi(z, w) = a(z, w) - 1 = w - 1. \quad (14)$$

For the spatial-temporal random HRM, we can prove that $z_2(w) = q^2/(q^2 + 1)$ and $\varphi[z_2(w), w] = w - 1$, as consistent with the conjectures [69]. To further test the conjectures, we numerically calculate four chaotic circuit models. For the spatial-temporal random case, we test the HRM and RPM after ensemble averages, and for the spatial-temporal invariant case, we test the 3PM and the Z_2 -COE model. All four models agree with our conjecture excellently, as shown in Fig. 2. The results also confirm that the LLGs are generally non-diagonalizable, and thus, one cannot even numerically obtain all eigenvalues accurately. For the integrable model XYZc, the conjectures are indeed violated as shown by the inset of Fig. 2. Numerically, we find that the leading eigenvalue of $F_w^{(22)}$ is $z_2(w = 1)$, resulting in much larger Jordan blocks. For the XYZc, we empirically find that $\varphi[z_2(w), w] = 2(w - 1)$, as verified in Fig. 2.

Leading singular value approximation.— Under Conjecture 2, there is a unique pair of leading singular states that dominates the LLGs in the large τ limit [69],

$$\lim_{\tau \rightarrow \infty} \|\lambda_{w, \tau}^{-1} F_{L, w}^\tau - |\lambda_{w, \tau}^L\rangle\langle\lambda_{w, \tau}^R|\| = 0, \quad (15)$$

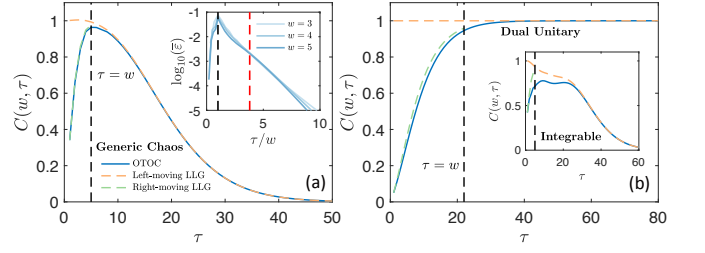


FIG. 3. Testing the LSVA. (a) OTOC of the spatial-temporal invariant 3PM with $w = 5$ for one realization. The inset shows the error of the LSVA, $\varepsilon = |C - C_{\text{LSVA}}|$, averaged over 25 realizations, as a function of w . The red dashed line here is the putative position of the butterfly cone obtained in [69]. (b) OTOC of the spatial-temporal random DU circuits with $w = 22$, and the dashed lines represent the LSVA. The inset shows the OTOC and the LSVA for the XYZc model with $w = 5$.

where $\lambda_{w, \tau}$ is the leading singular value of $F_{L, w}^\tau$ with its left and right singular states $\langle\lambda_{w, \tau}^L|, |\lambda_{w, \tau}^R\rangle$. Thus, the OTOC is exactly controlled by the leading singular value in this limit. Therefore, we introduce the leading singular value approximation (LSVA) for the left-moving LLG,

$$C_{\text{LSVA}}(w, \tau) := -\lambda_{w, \tau} \langle L_w | \lambda_{w, \tau}^L \rangle \langle \lambda_{w, \tau}^R | R_w \rangle, \quad (16)$$

and conjecture that the LSVA describes the generic behavior of the OTOC. The C_{LSVA} of the right-moving LLG can be similarly defined.

In contrast, for small $\tau < w/\alpha$, the leading singular value is around q^w , and the singular states are approximated by the two bell states $-|0^w\rangle, |1^w\rangle$. In this region, the LSVA can be approximated by

$$C_{\text{LSVA}} \approx q^w \langle L_w | 0^w \rangle \langle 1^w | R_w \rangle = 1, \quad (17)$$

as shown by the orange lines in Fig. 3. The discrepancy is due to the finite- w effect. However, for $\tau \ll w/\alpha$, though the other singular values are exponentially smaller than the leading one, there are exponentially many of them, which cancel out the contributions to OTOC from the leading singular value. Nonetheless, most of the singular values decay exponentially with respect to τ , while the leading one is still around q^w . Consequently, the leading singular value becomes dominant around $\tau \approx w$, resulting in the “1” region (and the second “0” region) of the OTOC. Particularly, we analytically and numerically show in the spatial-temporal random HRM that the leading singular value captures the behavior of the OTOC [69]. Although the leading singular value of the left-moving LLG cannot explain the first “0” region $\tau \lesssim w$, it can be explained by the right-moving LLG whose leading singular value dominates in this region. In Fig. 3(a), we study the spatial-temporal invariant 3PM, whose OTOC is well described by the LSVA. Further, we find that the LSVA works well for any typical realization and is more accurate in an increasingly large region in τ ,

as shown in the inset of Fig. 3(a). However, the LSVA does not agree with the OTOC of the integrable model within the butterfly cone, as shown in Fig. 3(b), but it indeed captures the behavior at the wavefront.

Leading singular state.— Under Conjecture 2, we can obtain the asymptotic behavior for the leading singular states in the large τ limit. As there is only one leading Jordan block, the leading singular states are simply given by a single pair of left and right eigenstates of that block. For LLG, these eigenstates can always be generated from $F_{w=1}$ using Eq. (7), we derive [69]

$$\begin{aligned} \lim_{\tau \rightarrow \infty} |\lambda_{w,\tau}^L\rangle &\propto |0^{w-1}\rangle \otimes_k |z_2^R\rangle, \\ \lim_{\tau \rightarrow \infty} \langle \lambda_{w,\tau}^R| &\propto \langle z_2^L| \otimes_k \langle 1^{w-1}|, \end{aligned} \quad (18)$$

where $\langle z_2^L|, |z_2^R\rangle$ are the left and right leading eigenstates of $F_{L,w=1}$ respectively. Similar to the singular states in small τ and large w , the leading singular states are product states of $|0\rangle$ -s or $|1\rangle$ -s, except for one site. Hence, a natural ansatz for the leading singular states is $|\lambda_{w,\tau}^{L,VP}\rangle = |0^{w-1}\rangle \otimes |v_L(\tau)\rangle$ and $\langle \lambda_{w,\tau}^{R,VP}| = \langle v_R(\tau)| \otimes \langle 1^{w-1}|$, where $\langle v_R(\tau)|, |v_L(\tau)\rangle$ are obtained through the variational principle, giving a computational advantage over the singular value decomposition. In Sec. III C of [69], we numerically show that the variational ansatz approximates the OTOC of the spatial-temporal invariant 3PM with good precision.

Dual unitarity and its perturbation.— Here we comment on the differences among the LLGs for generic chaos, DU and its perturbation [41, 64–66, 68]. First, the operator norms of the LLGs for DU circuits are drastically different from those of generic chaotic circuits. Particularly, it is analytically known that $\|T_w^\tau\| = 1$ and $\|F_w^\tau\| = q^w$, which, along with the singular states, are τ -independent. Consequently, the OTOC cannot grow or decay exponentially along the LL direction. Second, it can be proved that $a(z) = g(z)$ for eigenvalues z with unit modulus [69]. As the leading eigenvalue of F_w is $z_2(w) = 1$, we have $g(z_2, w) = a(z_2, w) \geq w$. Additionally, the LLG of DU circuits is always block-diagonal instead of an upper-triangular one, though each block may be non-Hermitian. Note that the LSVA also works for DU circuits as shown in Fig. 3(b), but the leading singular value behaves differently in contrast to the generic chaos case. Lastly, the generic chaotic case has been explored by weakly-perturbing a DU model in the so-called maximally-chaotic subspace (MCS) [68], giving results coinciding with Eq. (10) and Eq. (12) in the LLG projected onto the MCS. However, we find that MCS are generally not invariant subspaces in generic chaotic models, and the approximation of OTOC using MCS in spatial-temporal invariant circuits becomes increasingly less accurate as the LLG size, w increases. See comparison and numerics in [69].

Conclusion.— In this work, we study the OTOC for generic many-body quantum chaotic circuit models

in terms of LLGs. We demonstrate that the OTOC can be approximated by the leading singular value of the LLG. Using symmetries and recursivity of the LLG, we propose two conjectures on the universal aspects of generic many-body quantum chaotic circuits, Eq. (11) and Eq. (12), which are numerically tested using the large- τ decay of the OTOC. Understanding further implications of symmetries and recursivity of the LLG, studying behaviors of OTOC and LLG in the presence of local conserved quantities, and the construction of analogs of the LLG in relativistic quantum field theory are natural open directions for future studies.

Acknowledgement.— After the upload of this work, we are grateful for a discussion with Pieter Claeys and Michael Rampp which allowed us to clarify the similarities and differences between [68] and this work, see [69]. We are grateful to John Chalker, Andrea De Luca, Austen Lamacraft, Henning Schomerus, and Saumya Shivam for discussions and previous collaborations. This work is supported by the Research Grants Council of Hong Kong (Grants No. CityU 21304720, No. CityU 11300421, No. CityU 11304823, and No. C7012-21G) and City University of Hong Kong (Projects No. 9610428 and No. 7005938). A.C. acknowledges the support from the Royal Society grant RGS\R1\231444, and the fellowships from the Croucher Foundation and the PCTS at Princeton University. D.A.H. is supported in part by NSF QLCI grant OMA-2120757. K.H. is also supported by the Hong Kong PhD Fellowship Scheme.

* xiao.li@cityu.edu.hk

† amos.chan@lancaster.ac.uk

- [1] J. M. Deutsch, *Phys. Rev. A* **43**, 2046 (1991).
- [2] M. Srednicki, *Phys. Rev. E* **50**, 888 (1994).
- [3] M. Rigol, V. Dunjko, and M. Olshanii, *Nature* **452**, 854 (2008).
- [4] J. Maldacena, S. H. Shenker, and D. Stanford, *J. High Energy Phys.* **2016**, 106.
- [5] S. H. Shenker and D. Stanford, *J. High Energy Phys.* **2014**, 67.
- [6] A. I. Larkin and Y. N. Ovchinnikov, *Sov. Phys. JETP* **28**, 1200 (1969).
- [7] J. Li, R. Fan, H. Wang, B. Ye, B. Zeng, H. Zhai, X. Peng, and J. Du, *Phys. Rev. X* **7**, 031011 (2017).
- [8] M. Gärttner, J. G. Bohnet, A. Safavi-Naini, M. L. Wall, J. J. Bollinger, and A. M. Rey, *Nat. Phys.* **13**, 781 (2017).
- [9] K. A. Landsman, C. Figgatt, T. Schuster, N. M. Linke, B. Yoshida, N. Y. Yao, and C. Monroe, *Nature* **567**, 61 (2019).
- [10] M. K. Joshi, A. Elben, B. Vermersch, T. Brydges, C. Maier, P. Zoller, R. Blatt, and C. F. Roos, *Phys. Rev. Lett.* **124**, 240505 (2020).
- [11] M. Blok, V. Ramasesh, T. Schuster, K. O’Brien, J. Kreikebaum, D. Dahlen, A. Morvan, B. Yoshida, N. Yao, and I. Siddiqi, *Phys. Rev. X* **11**, 021010 (2021).

- [12] X. Mi, P. Roushan, C. Quintana, S. Mandrà, J. Marshall, C. Neill, F. Arute, K. Arya, J. Atalaya, R. Babbush, J. C. Bardin, R. Barends, J. Basso, A. Bengtsson, S. Boixo, A. Bourassa, M. Broughton, B. B. Buckley, D. A. Buell, B. Burkett, N. Bushnell, Z. Chen, B. Chiaro, R. Collins, W. Courtney, S. Demura, A. R. Derk, A. Dunsworth, D. Eppens, C. Erickson, E. Farhi, A. G. Fowler, B. Foxen, C. Gidney, M. Giustina, J. A. Gross, M. P. Harrigan, S. D. Harrington, J. Hilton, A. Ho, S. Hong, T. Huang, W. J. Huggins, L. B. Ioffe, S. V. Isakov, E. Jeffrey, Z. Jiang, C. Jones, D. Kafri, J. Kelly, S. Kim, A. Kitaev, P. V. Klimov, A. N. Korotkov, F. Kostritsa, D. Landhuis, P. Laptev, E. Lucero, O. Martin, J. R. McClean, T. McCourt, M. McEwen, A. Megrant, K. C. Miao, M. Mohseni, S. Montazeri, W. Mruczkiewicz, J. Mutus, O. Naaman, M. Neeley, M. Newman, M. Y. Niu, T. E. O'Brien, A. Opremcak, E. Ostby, B. Pato, A. Petukhov, N. Redd, N. C. Rubin, D. Sank, K. J. Satzinger, V. Shvarts, D. Strain, M. Szalay, M. D. Trevithick, B. Villalonga, T. White, Z. J. Yao, P. Yeh, A. Zalcman, H. Neven, I. Aleiner, K. Kechedzhi, V. Smelyanskiy, and Y. Chen, *Science* **374**, 1479 (2021).
- [13] J. Braumüller, A. H. Karamlou, Y. Yanay, B. Kannan, D. Kim, M. Kjaergaard, A. Melville, B. M. Niedzielski, Y. Sung, A. Vepsäläinen, R. Winik, J. L. Yoder, T. P. Orlando, S. Gustavsson, C. Tahan, and W. D. Oliver, *Nat. Phys.* **18**, 172 (2021).
- [14] K. Hashimoto, K. Murata, and R. Yoshii, *J. High Energy Phys.* **2017** (10).
- [15] E. B. Rozenbaum, S. Ganeshan, and V. Galitski, *Phys. Rev. Lett.* **118**, 086801 (2017).
- [16] D. J. Luitz and Y. Bar Lev, *Phys. Rev. B* **96**, 020406 (2017).
- [17] C.-J. Lin and O. I. Motrunich, *Phys. Rev. B* **97**, 144304 (2018).
- [18] I. Garcí a-Mata, M. Saraceno, R. A. Jalabert, A. J. Roncaglia, and D. A. Wisniacki, *Phys. Rev. Lett.* **121**, 210601 (2018).
- [19] J. Rammensee, J. D. Urbina, and K. Richter, *Phys. Rev. Lett.* **121**, 124101 (2018).
- [20] S. Pappalardi, A. Russomanno, B. Ž unko vič, F. Iemini, A. Silva, and R. Fazio, *Phys. Rev. B* **98**, 134303 (2018).
- [21] B. Swingle, *Nat. Phys.* **14**, 988 (2018).
- [22] C. B. Dağ, K. Sun, and L.-M. Duan, *Phys. Rev. Lett.* **123**, 140602 (2019).
- [23] J. Chá vez-Carlos, B. L. del Carpio, M. A. Bastarrachea-Magnani, P. Stránský, S. Lerma-Herná ndez, L. F. Santos, and J. G. Hirsch, *Phys. Rev. Lett.* **122**, 024101 (2019).
- [24] T. Xu, T. Scaffidi, and X. Cao, *Phys. Rev. Lett.* **124**, 140602 (2020).
- [25] J. c. v. Bensa and M. Ž nidarič, *Phys. Rev. Res.* **4**, 013228 (2022).
- [26] Y. Gu, A. Kitaev, and P. Zhang, *J. High Energy Phys.* **2022**, 133.
- [27] T. Zhou and B. Swingle, *Nat. Commun.* **14**, 3411 (2023).
- [28] P. Martinez-Azcona, A. Kundu, A. del Campo, and A. Chenu, Unveiling out-of-time-order correlators from stochastic operator variance (2023), [arXiv:2302.12845 \[quant-ph\]](https://arxiv.org/abs/2302.12845).
- [29] V. Balachandran, L. F. Santos, M. Rigol, and D. Poletti, *Phys. Rev. B* **107**, 235421 (2023).
- [30] A. Nahum, J. Ruhman, S. Vijay, and J. Haah, *Phys. Rev. X* **7**, 031016 (2017).
- [31] C. W. von Keyserlingk, T. Rakovszky, F. Pollmann, and S. L. Sondhi, *Phys. Rev. X* **8**, 021013 (2018).
- [32] A. Nahum, S. Vijay, and J. Haah, *Phys. Rev. X* **8**, 021014 (2018).
- [33] T. Rakovszky, F. Pollmann, and C. W. von Keyserlingk, *Phys. Rev. X* **8**, 031058 (2018).
- [34] V. Khemani, A. Vishwanath, and D. A. Huse, *Phys. Rev. X* **8**, 031057 (2018).
- [35] A. Chan, A. De Luca, and J. T. Chalker, *Phys. Rev. X* **8**, 041019 (2018).
- [36] A. Chan, A. De Luca, and J. T. Chalker, *Phys. Rev. Lett.* **121**, 060601 (2018).
- [37] B. Bertini, P. Kos, and T. Prosen, *Phys. Rev. Lett.* **121**, 264101 (2018).
- [38] B. Bertini, P. Kos, and T. Prosen, *Phys. Rev. Lett.* **123**, 210601 (2019).
- [39] A. J. Friedman, A. Chan, A. De Luca, and J. T. Chalker, *Phys. Rev. Lett.* **123**, 210603 (2019).
- [40] T. Zhou and A. Nahum, *Phys. Rev. B* **99**, 174205 (2019).
- [41] B. Bertini, P. Kos, and T. Prosen, *SciPost Phys.* **8**, 67 (2020).
- [42] Y. Li, X. Chen, and M. P. A. Fisher, *Phys. Rev. B* **98**, 205136 (2018).
- [43] B. Skinner, J. Ruhman, and A. Nahum, *Phys. Rev. X* **9**, 031009 (2019).
- [44] Y. Li, X. Chen, and M. P. A. Fisher, *Phys. Rev. B* **100**, 134306 (2019).
- [45] M. J. Gullans and D. A. Huse, *Phys. Rev. X* **10**, 041020 (2020).
- [46] Y. Bao, S. Choi, and E. Altman, *Phys. Rev. B* **101**, 104301 (2020).
- [47] C.-M. Jian, Y.-Z. You, R. Vasseur, and A. W. W. Ludwig, *Phys. Rev. B* **101**, 104302 (2020).
- [48] A. Zabalo, M. J. Gullans, J. H. Wilson, S. Gopalakrishnan, D. A. Huse, and J. H. Pixley, *Phys. Rev. B* **101**, 060301 (2020).
- [49] P. Saad, S. H. Shenker, and D. Stanford, A semiclassical ramp in syk and in gravity (2019), [arXiv:1806.06840 \[hep-th\]](https://arxiv.org/abs/1806.06840).
- [50] H. Gharibyan, M. Hanada, S. H. Shenker, and M. Tezuka, *J. High Energy Phys.* **2018**, 124.
- [51] D. Roy and T. c. v. Prosen, *Phys. Rev. E* **102**, 060202 (2020).
- [52] S. Moudgalya, A. Prem, D. A. Huse, and A. Chan, *Phys. Rev. Research* **3**, 023176 (2021).
- [53] A. Chan, A. De Luca, and J. T. Chalker, *Phys. Rev. Lett.* **122**, 220601 (2019).
- [54] L. Foini and J. Kurchan, *Phys. Rev. E* **99**, 042139 (2019).
- [55] M. Akila, D. Waltner, B. Gutkin, and T. Guhr, *J. Phys. A: Math. Theor.* **49**, 375101 (2016).
- [56] N. Hahn and D. Waltner, *Acta Phys. Pol. A* **136**, 841 (2019).
- [57] A. Chan, A. De Luca, and J. T. Chalker, *Phys. Rev. Res.* **3**, 023118 (2021).
- [58] S. J. Garratt and J. T. Chalker, *Phys. Rev. X* **11**, 021051 (2021).
- [59] A. Leroise, M. Sonner, and D. A. Abanin, *Phys. Rev. X* **11**, 021040 (2021).
- [60] M. Ippoliti, T. Rakovszky, and V. Khemani, *Phys. Rev. X* **12**, 011045 (2022).
- [61] T.-C. Lu and T. Grover, *PRX Quantum* **2**, 040319 (2021).
- [62] A. Chan, S. Shivam, D. A. Huse, and A. D. Luca, *Nat. Commun.* **13**, 7484 (2022).
- [63] S. Shivam, A. D. Luca, D. A. Huse, and A. Chan, *Phys. Rev. Lett.* **130**, 140403 (2023).

- [64] P. Kos, B. Bertini, and T. Prosen, Correlations in perturbed dual-unitary circuits: Efficient path-integral formula (2020), [arXiv:2006.07304](https://arxiv.org/abs/2006.07304) [[cond-mat.stat-mech](https://arxiv.org/abs/2006.07304)].
- [65] P. W. Claeys and A. Lamacraft, [Phys. Rev. Res. **2**, 033032 \(2020\)](https://doi.org/10.1103/PhysRevRes.2.033032).
- [66] B. Bertini and L. Piroli, [Phys. Rev. B **102**, 064305 \(2020\)](https://doi.org/10.1103/PhysRevB.102.064305).
- [67] P. W. Claeys, J. Herzog-Arbeitman, and A. Lamacraft, [SciPost Physics **12**, 10.21468/scipostphys.12.1.007 \(2022\)](https://doi.org/10.21468/scipostphys.12.1.007).
- [68] M. A. Rampp, R. Moessner, and P. W. Claeys, [Phys. Rev. Lett. **130**, 130402 \(2023\)](https://doi.org/10.1103/PhysRevLett.130.130402).
- [69] See supplementary material at [\[url\]](#) for the definitions of models, the proofs of the properties of the light-like generators, additional numerics on the w -dependence of the OTOC, the performance of the LSVA, and the variational method.

Supplemental Material for “Out-of-time-order correlator, many-body quantum chaos, light-like generators, and singular values”

CONTENTS

I. Quantum many-body models	1
A. Integrable model	1
B. Generic chaotic models	1
C. Dual unitarity (chaotic) model	2
D. Completely localized model	2
II. Level statistics	2
III. Reducibility and consequences	3
A. Algebraic multiplicity	3
B. Irreducibility of the leading singular state	3
C. A variational method for leading singular state	4
IV. Asymptotic decay rate	4
V. Spatial-temporal random HRM	5
A. Eigenvalues and multiplicity	5
B. Extracting butterfly velocity from leading singular value	5
VI. Light-like generators for two special cases	5
A. Dual unitary models	5
B. Completely localized models	6
VII. Difference between this work and perturbative results around DU limit in [5]	6
VIII. Mathematical proofs	7
A. Proof of $ \sigma_{\text{spectrum}}(T_w) \leq 1$	7
1. Large τ behaviour of T_w	7
2. Asymptotic behavior of the singular value	7
3. Proof of $\langle v_L T_w^\tau v_R \rangle < \infty$	8
4. Multiplicity of leading eigenvalues	8
B. Proof of $\ T_w\ \leq q$	9
C. Proof of $z_2(w) = z_2(w = 1)$	9
1. Main proof	9
2. Proof of Equation (S70)	10
D. Spatial-temporal random Haar-random model	11
1. Similar transformation	12
2. Eigenvalues	12
3. Geometric multiplicity of the subleading eigenvalue	13
4. Leading singular value around the butterfly cone	13
IX. Additional numerics	14
A. OTOC, LSVA, and the variation method in the spatial-temporal invariant models	14
B. OTOC, LSVA, and the variation method in the spatial-temporal random HRM	14
C. w -dependence of the large τ behavior	14

References

16

I. QUANTUM MANY-BODY MODELS

In this work, we focus on the quantum circuits with the brick-wall geometry as models of quantum many-body systems. Such models are defined with a evolution operator given by

$$U(t) = \prod_{s=1}^t \tilde{U}(s), \quad \tilde{U}(s) = \bigotimes_{i \in 2\mathbb{Z} + s \bmod 2} u_{i,i+1}. \quad (\text{S1})$$

For spatial-temporal invariant circuits, the two-site gates $u_{i,i+1}$ are identical for all i , while for spatial-temporal random circuits, $u_{i,i+1}$ are independent random variables drawn from the same ensemble. We consider 4 classes of spatial-temporal invariant or random models, as listed below.

A. Integrable model

We consider the following many-body integrable model with $q = 2$,

$$u_{XYZc} = \exp \left\{ i \sum_{\mu=x,y,z} a_\mu \sigma_\mu \otimes \sigma_\mu \right\}, \quad (\text{S2})$$

where σ_μ is the Pauli matrices, and we take $(a_x, a_y, a_z) = (0.3, 0.4, 0.5)$ in the main text. The model has three symmetries: the time-reversal symmetry $\{u_{XYZc}\}^T = u_{XYZc}$, the Z_2 symmetry $(\sigma_z \otimes \sigma_z) u_{XYZc} (\sigma_z \otimes \sigma_z) = u_{XYZc}$, and the particle-hole symmetry $(\sigma_x \otimes \sigma_x) u_{XYZc} (\sigma_x \otimes \sigma_x) = u_{XYZc}$.

B. Generic chaotic models

For generic many-body quantum chaotic models, we consider the spatial-temporal invariant or random Haar-random model (HRM) [1] and 3 parameter model (3PM) [2],

$$\begin{aligned} u_{\text{HRM}} &= U^{\text{CUE}}(q^2), \\ u_{\text{3PM}} &= [U_1^{\text{CUE}}(2) \otimes U_2^{\text{CUE}}(2)] u_{XYZc} \\ &\quad \times [U_3^{\text{CUE}}(2) \otimes U_4^{\text{CUE}}(2)], \end{aligned} \quad (\text{S4})$$

where $U_i^{\text{CUE/COE}}(n)$ are independent random matrices drawn from the circular unitary/orthogonal ensemble of degree n (CUE(n)/COE(n)). Here, the HRM is defined for generic q , while the 3PM is defined only for $q = 2$. We again take $(a_x, a_y, a_z) = (0.3, 0.4, 0.5)$ for the 3PM in the main text. We also consider the random phase model (RPM) [3] for generic q

$$u_{\text{RPM}} = [U_1^{\text{CUE}}(q) \otimes U_2^{\text{CUE}}(q)] \Phi$$

$$\times [U_3^{\text{CUE}}(q) \otimes U_4^{\text{CUE}}(q)], \quad (\text{S5})$$

where $[\Phi]_{\mu\nu}^{\mu'\nu'} = \delta_{\mu}^{\mu'} \delta_{\nu}^{\nu'} e^{i\phi_{\mu\nu}}$, and $\phi_{\mu\nu}$ are independent random variables drawn from a normal distribution with zero mean and variance ϵ . In the main text, we take $q = 4$ and $\epsilon = 1$. Further, we consider the Z_2 -COE model with $q = 2$ because it also has the same Z_2 and time-reversal symmetries as the XYZc model, given by

$$u_{Z_2\text{-COE}} = \begin{bmatrix} [U_1^{\text{COE}}(2)]_{11} & 0 & [U_1^{\text{COE}}(2)]_{12} \\ 0 & U_2^{\text{COE}}(2) & 0 \\ [U_1^{\text{COE}}(2)]_{21} & 0 & [U_1^{\text{COE}}(2)]_{22} \end{bmatrix}, \quad (\text{S6})$$

where $[U]_{jk}$ denotes the j, k entry of the matrix.

C. Dual unitarity (chaotic) model

For dual unitary (DU) chaotic model [4], we consider the $q = 2$ case, and the model is given by

$$u_{\text{DU}} = [U_1^{\text{CUE}}(2) \otimes U_2^{\text{CUE}}(2)] u_{\text{XYZc}} \times [U_3^{\text{CUE}}(2) \otimes U_4^{\text{CUE}}(2)]$$

with $(a_x, a_y) = (\pi/4, \pi/4)$ and arbitrary a_z . In the main text, we take $a_z = 0.5$. The DU model considered here belongs to the ‘‘completely chaotic’’ DU circuits, which is the generic case within the DU family [4]. Importantly, such unitary 2-site gates satisfy for following relations,

$$\begin{aligned} u_{cd'}^{ab'}(u^*)_{a'b'}^{c'd'} &= \delta_{a,a'} \delta_{c,c'}, \\ u_{c'd}^{a'b'}(u^*)_{a'b'}^{c'd'} &= \delta_{b,b'} \delta_{d,d'}, \end{aligned} \quad (\text{S7})$$

which means that unitarity also holds in the spatial direction.

D. Completely localized model

The completely localized model for generic q is taken as

$$u_{\text{loc}} = U^{\text{CUE}}(q) \otimes U^{\text{CUE}}(q), \quad (\text{S8})$$

i.e., the two-site unitary gates do not couple the two sites.

II. LEVEL STATISTICS

Here we consider the level statistics of space-like generators or ‘‘Floquet operators’’ which generate the dynamics of the system in the time direction. Generally, the level statistics of the (space-like) Floquet operator for a chaotic system follows the ones of Hermitian random matrix theory, like CUE or COE, whereas it may manifest other level statistics in the presence of space-time translational symmetry. We say that a Floquet system has space-time translational (STT) symmetry if its evolution operator $U(t_2, t_1)$ satisfies

$$\mathcal{T}U(t_2, t_1)\mathcal{T}^{-1} = U(t_2 + T/n, t_1 + T/n), \quad (\text{S9})$$

where \mathcal{T} is the translation by one site, T is the period of the Floquet system, and n is a positive integer. Note that $n = 2$ for the brick-wall structure studied in this work. Thus, the STT symmetry spontaneously implies that

$$\mathcal{T}^n U(t_2, t_1) \mathcal{T}^{-n} = U(t_2 + T, t_1 + T) = U(t_2, t_1), \quad (\text{S10})$$

that is, the system is invariant under translation by n sites. Additionally, the Floquet operator in this system is reduced to

$$\begin{aligned} F &= U(T, T - T/n) \times \cdots \times U(T/n, 0) \\ &= \mathcal{T}^{(n-1)} U_0 \mathcal{T}^{-(n-1)} \times \mathcal{T}^{(n-2)} U_0 \mathcal{T}^{-(n-2)} \times \cdots \times U_0 \\ &= \mathcal{T}^n (\mathcal{T}^{-1} U_0)^n = (\mathcal{T}^{-1} U_0)^n \mathcal{T}^n, \end{aligned} \quad (\text{S11})$$

where $U_0 = U(T/n, 0)$. In a given momentum subspace, \mathcal{T}^n is constant, and therefore, we only need to consider

$$F' = (\mathcal{T}^{-1} U_0)^n. \quad (\text{S12})$$

If F' is chaotic, then $\mathcal{T}^{-1} U_0$ should not be integrable because the power of an integrable operator is still integrable. However, if $\mathcal{T}^{-1} U_0$ is chaotic and we assume it to follow CUE or COE, F' cannot be described by CUE or COE. Instead, F' should be CUE^n or COE^n which is defined as

$$\text{CUE}^n := \{S^n : S \in \text{CUE}\},$$

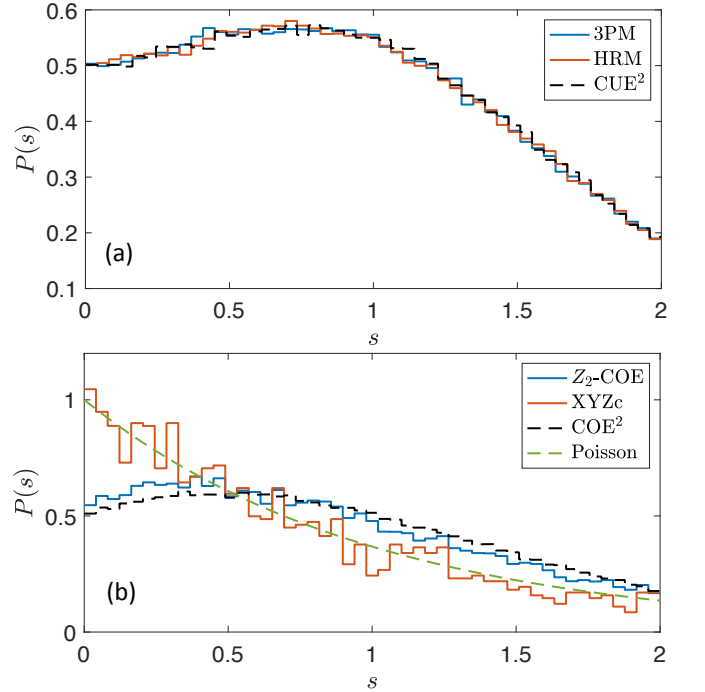


FIG. S1. Spacing distribution $P(s)$ of the spatial-temporal invariant models. (a) Two models without Z_2 and time-reversal symmetries. The system size is $L = 14$, and the results are averaged over 100 realizations. (b) Two models with Z_2 and time-reversal symmetries. The system size is $L = 16$, and the result of the Z_2 -COE model is averaged over 10 realizations. Here, the results are in the $(2\pi/L)$ -momentum sector and parity-even sector if Z_2 symmetry exists. What is more, we also resolve the particle-hole symmetry for the XYZc model. For the CUE^2 and COE^2 matrices, the result is averaged over 100 realizations of 2000×2000 matrices.

$$\text{COE}^n := \{S^n : S \in \text{COE}\}. \quad (\text{S13})$$

Particularly, we verify the CUE² and COE² by studying the level statistics in the spatial-temporal invariant 3PM, HRM, and Z_2 -COE model as shown in Fig. S1. For the XYZc model, the level statistics indicates that it is integrable.

III. REDUCIBILITY AND CONSEQUENCES

A. Algebraic multiplicity

Nondiagonalizability appears only if there are degeneracies (algebraic multiplicity greater than 1). In this section, we show that the degeneracies result from the reducibility introduced in the main text. To start, we consider the block-upper-diagonal structure ($w \geq 2$) shown in the main text,

$$F_w = \begin{bmatrix} \tilde{F}_{w-1}^{(11)} & \tilde{F}_w^{(12)} & \tilde{F}_{w-1}^{(13)} & \tilde{F}_w^{(14)} \\ 0 & \tilde{F}_w^{(22)} & 0 & \tilde{F}_w^{(24)} \\ 0 & 0 & \tilde{F}_{w-2}^{(33)} & \tilde{F}_{w-1}^{(34)} \\ 0 & 0 & 0 & \tilde{F}_{w-1}^{(44)} \end{bmatrix}. \quad (\text{S14})$$

See Fig. S2 for the diagrammatical representation of a few blocks as examples. It is easy to see that for $w > 2$, $\tilde{F}_{w-2}^{(33)}$ is isomorphic to F_{w-2} , and therefore they have the same eigenvalues. For $w = 2$, $\tilde{F}_{w-2}^{(33)}$ is trivially zero. Similarly, there is another isomorphism,

$$F_{w-1} \cong \begin{bmatrix} \tilde{F}_{w-1}^{(11)} & \tilde{F}_{w-1}^{(13)} \\ 0 & \tilde{F}_{w-2}^{(33)} \end{bmatrix} \cong \begin{bmatrix} \tilde{F}_{w-2}^{(33)} & \tilde{F}_{w-1}^{(34)} \\ 0 & \tilde{F}_{w-1}^{(44)} \end{bmatrix}. \quad (\text{S15})$$

Hence, the algebraic multiplicity of $z \neq 0$ in $\tilde{F}_{w-1}^{(11)}, \tilde{F}_{w-1}^{(44)}$ is $a(z, w-1) - a(z, w-2)$, and adding up four diagonal blocks, we obtain the recursive relation for $w \geq 2$,

$$a(z, w) = 2a(z, w-1) - a(z, w-2) + \tilde{a}(z, w). \quad (\text{S16})$$

Next, using Eq. (S16), we will prove that if z is an eigenvalue of w , then $a(z, w+1) \geq a(z, w) + 1$. Suppose z is an eigenvalue of F_{w_0} but not F_{w_0-1} for some w_0 . If $w_0 = 1$, then we have

$$\begin{aligned} a(z, w_0 + 1) &= 2a(z, w_0) + \tilde{a}(z, w_0 + 1) \\ &\geq a(z, w_0) + 1, \end{aligned} \quad (\text{S17})$$

where we use the fact that $\tilde{F}_0^{(33)} = 0$. If $w_0 > 1$, then we have $a(z, w_0 - 1) = 0$ and we have also Eq. (S17). Hence, we have

$$\begin{aligned} a(z, w) - a(z, w-1) &\geq a(z, w-1) - a(z, w-2) \\ &\geq a(z, w_0 + 1) - a(z, w_0) \geq 1. \end{aligned} \quad (\text{S18})$$

Note that the equality holds if $\tilde{a}(z, w) = 0$ for all $w > w_0$.

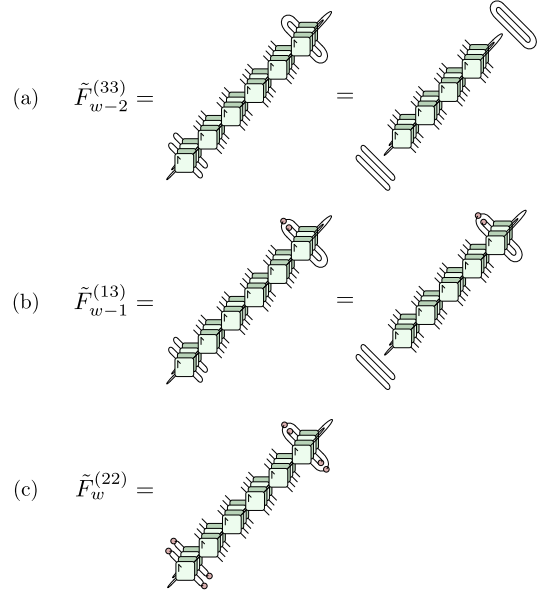


FIG. S2. Three example blocks in Eq. (S14), where red dots represent operators that are orthogonal to the identity operator.

B. Irreducibility of the leading singular state

In Section VIII A 1, we prove that the OTOC possesses the following scaling

$$\limsup_{\tau \rightarrow \infty} \frac{C(w, \tau)}{\tau^{\varphi[z_2(w), w]} |z_2(w)|^\tau} < +\infty, \quad (\text{S19})$$

where $\varphi(z, w) = N_{\max}(z, w) - 1$, and $N_{\max}(z, w)$ is the dimension of the largest Jordan block corresponding to eigenvalue z . What is more, the limit is nonvanishing if the initial and final states have nonvanishing overlap with the leading singular states. If there only one Jordan block corresponding to $z_2(w)$ for all w , then we have $\varphi[z_2(w), w] = a[z_2(w), w] - 1$ and the scaling is greater for larger w , because either the algebraic multiplicity of $z_2(w-1)$ increases or $z_2(w)$ is greater than $z_2(w-1)$. Hence, we have $C(w, \tau) \gg C(w-1, \tau)$ in the large τ limit unless the initial and final states of $C(w, \tau)$ have nonvanishing overlap with the leading singular states. Consider an arbitrary pair of initial and final states $|v_R\rangle, \langle v_L|$ of width $(w-1)$, and we have

$$\begin{aligned} C(w-1, \tau) &= \langle v_L | F_{w-1}^\tau | v_R \rangle \\ &= \langle v'_L | F_w^\tau | v'_R \rangle = C'(w, \tau), \end{aligned} \quad (\text{S20})$$

where

$$\langle v'_L | = \langle v_L | \otimes \langle 1 |, \quad |v'_R\rangle = |v_R\rangle \otimes |v\rangle. \quad (\text{S21})$$

Hence, $|v\rangle$ is an arbitrary state satisfying $\langle 1 | v \rangle = 1$. If $\langle v'_R |, \langle v'_L |$ have nonvanishing overlap with the lead singular states, then $C'(w, \tau) \gg C(w, \tau)$ for large enough τ , which is impossible. As $|v_L\rangle$ and $|v_R\rangle$ are both arbitrary, the only way to have vanishing overlap is that $(\langle v_L | \otimes_r \langle 1 |) | \lambda_L \rangle = 0$ for all $\langle v_L |$, which is just the definition of “irreducibility for bra states”. Similarly, we can show that $|\lambda_R\rangle$ is also irreducible.

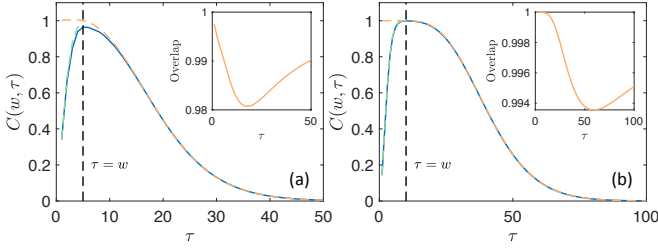


FIG. S3. OTOC in (a) spatial-temporal invariant 3PM with $w = 5$ for one realization, (b) spatial-temporal random HRM with $w = 10$ and $q = 2$. Here, the blue lines represent the exact results, the orange lines use the left-moving LL generator, and the green lines use the right-moving one. The inset shows the overlap between the exact leading singular state and the variational ansatz $|\langle \lambda_{w,\tau}^{L,VP} | \lambda_{w,\tau}^L \rangle \langle \lambda_{w,\tau}^{R,VP} | \lambda_{w,\tau}^R \rangle|$.

For instance, if we further assume $z_2(w) = z_2(w = 1)$, utilizing Eq. (S49), we have

$$\begin{aligned} \langle \lambda_{\tau=\infty}^L | &\propto \langle z_2^R(w) | = \langle 0^{w-1} | \otimes_r \langle z_2^R(w = 1) |, \\ | \lambda_{\tau=\infty}^R \rangle &\propto | z_2^L(w) \rangle = | z_2^L(w = 1) \rangle \otimes_r | 1^{w-1} \rangle, \end{aligned} \quad (\text{S22})$$

where $\langle z_2^L(w) |, | z_2^R(w) \rangle$ are the left and right eigenstate of eigenvalue $z_2(w)$ respectively. Incorporating Eq. (S49), we can readily verify the irreducibility because $\langle 1 | z_2^R(w = 1) \rangle = \langle 0 | z_2^L(w = 1) \rangle = 0$.

C. A variational method for leading singular state

In the main text, we devise the following variational ansatz for the leading singular states,

$$\begin{aligned} | \lambda_{w,\tau}^{L,VP} \rangle &= | 0^{w-1} \rangle \otimes | v_L(\tau) \rangle \\ \langle \lambda_{w,\tau}^{R,VP} | &= \langle v_R(\tau) | \otimes \langle 1^{w-1} |, \end{aligned} \quad (\text{S23})$$

where $\langle v_R(\tau) |, | v_L(\tau) \rangle$ are obtained variationally. In Fig. S3, we numerically show that the variational ansatz approximates the OTOC of the spatial-temporal invariant 3PM and the spatial-temporal random HRM with good precision. The high overlap between the variational state and the exact singular state also indicates that the ansatz indeed captures the primary structure of the leading singular states in generic models.

IV. ASYMPTOTIC DECAY RATE

According to Section VIII A 1, we know that the decay rate of the OTOC along LL direction is $z_2(w) + \varphi(w) \ln(\tau)/\tau$, which becomes $z_2(w)$ in the large τ limit. As illustrated in Fig. S4, the operator B moves along the LL direction, and the decay rate is thus $z_2(w)$. Particularly, the decay rate is $z_2(w = 1)$ if B is exactly on the lightcone of the operator $A(t)$. From the reducibility of the LLG, we have $z_2(w) \geq z_2(w = 1)$, so the decay rate is not less than $z_2(w = 1)$ for B inside the lightcone. Nonetheless, we will show that the $z_2(w = 1)$ is

asymptotically the maximal decay rate of the system, meaning that $z_2(w) = z_2(w = 1)$.

We can decompose $A(t)$ into Pauli strings,

$$A(t) = \sum_{x=-t}^{+\infty} A_x(t), \quad (\text{S24})$$

where $A_x(t)$ denotes the component of $A(t)$ that is supported on $[x, +\infty]$ and not identity on site x . It is obvious that only $A_x(t)$ with $x \in [-\tau, w' - \tau]$ contributes to $C(w', \tau)$, and therefore $C(w, \tau)$ and $C(w - 1, \tau)$ can be estimated by

$$\begin{aligned} C(w - 1, \tau) &\sim \sum_{x=-\tau}^{w-\tau-1} \|A_x(t)\|_F^2, \\ C(w, \tau) &\sim \|A_{w-\tau}(t)\|_F^2 + \sum_{x=-\tau}^{w-\tau-1} \|A_x(t)\|_F^2 \end{aligned} \quad (\text{S25})$$

If $z_2(w) > z_2(w - 1)$ for some w , then $C(w, \tau) \gg C(w', \tau)$ in the large τ limit for all $w' < w$. It means that

$$\|A_{w-\tau}(t)\|_F^2 \gg \sum_{x=-\tau}^{w-\tau-1} \|A_x(t)\|_F^2, \quad (\text{S26})$$

and that the OTOC between $A(t)$ and B is dominated by the OTOC between $A_{w-\tau}(t)$ and B . However, as B is exactly on the lightcone of $A_{w-\tau}(t)$, the asymptotic decay rate of the OTOC between $A(t)$ and B cannot be greater than $z_2(w = 1)$, leading to a contradiction. Hence, $z_2(w)$ should equal $z_2(w - 1)$ instead. In Section VIII C, this argument is rigorously proved under a mild assumption.

Note that Eq. (S26) is true as long as $C(w, \tau)$ has a greater scaling than $C(w - 1, \tau)$. Therefore, if $z_2(w) = z_2(w - 1)$ but $\varphi[z_2(w), w] > \varphi[z_2(w - 1), w - 1]$, Eq. (S26) also holds true. Notwithstanding, there is no contradiction because $\varphi[z_2(w), w]$ does not affect the asymptotic decay rate. For generic chaotic models, our conjecture implies an increase of $\varphi[z_2(w), w]$, and $\|A_{w-\tau}(t)\|_F^2 / \|A_{w-\tau-1}(t)\|_F^2$ should scale linearly with respect to t , instead of an exponential of t .

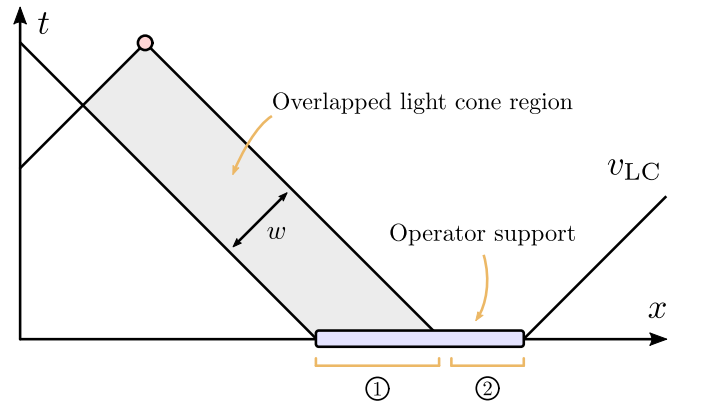


FIG. S4. OTOC of operator A (blue) with large operator support and B (red) with local operator support only depend on the overlapped light cone region with width w .

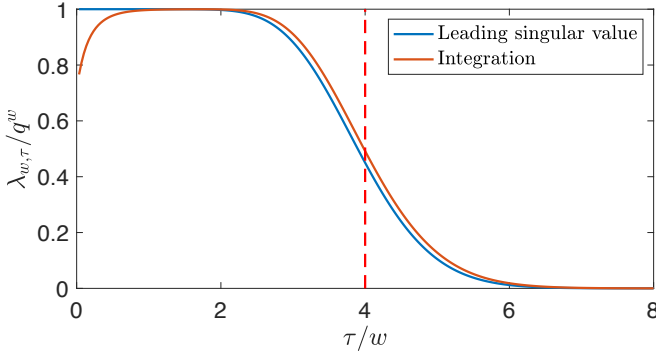


FIG. S5. Leading singular value of F_w in the spatial-temporal random HRM and the approximation Eq. (S31). The red dashed line denotes the position of the butterfly cone $\tau/w = q^2$. Here, we take $w = 30$ and $q = 2$.

V. SPATIAL-TEMPORAL RANDOM HRM

A. Eigenvalues and multiplicity

For the spatial-temporal random circuit, the ensemble-averaged LLG is given by

$$T_w = (0 | \overline{\bigcirc_r^w} \mathcal{U}_2 | 1) = (0 | \overline{\bigcirc_r^w} \overline{\mathcal{U}_2} | 1), \quad (\text{S27})$$

where the overline denotes the ensemble average. For the second equality, we use the fact that \mathcal{U}_2 s are independent random variables. In this section, we study the spatial-temporal random HRM, whose $\overline{\mathcal{U}_2}$ is given by

$$\overline{\mathcal{U}_2} = \tilde{M}_{j_1 j_2}^{i_1 i_2} |i_1\rangle |j_1\rangle \langle i_2| \langle j_2|, \quad (\text{S28})$$

where $\tilde{M}_{j_1 j_2}^{i_1 i_2} = \delta^{i_1 i_2} \delta_{j_1 j_2} q^2 \text{Wg}(i_1, j_1, q^2)$, and

$$\text{Wg}(i, j, N) = \begin{cases} (N^2 - 1)^{-1}, & i = j \\ -[N(N^2 - 1)]^{-1}, & i \neq j. \end{cases} \quad (\text{S29})$$

We prove in Section VIII D that the eigenvalues of the LLG are

$$\varepsilon_n = \begin{cases} \left(\frac{q}{q^2+1}\right)^n & n \text{ even,} \\ q \left(\frac{q}{q^2+1}\right)^n & n \text{ odd,} \end{cases} \quad (\text{S30})$$

with algebraic multiplicity $\binom{w}{n}$. Here, n takes value from $0, 1, \dots, w-1$. Further, the geometric multiplicity of the subleading eigenvalue $z_2 = q^2/(q^2+1)$ is one.

B. Extracting butterfly velocity from leading singular value

In Section VIII D, using Stirling's formula, we also show that the leading singular value of F_w around the butterfly cone is approximated by

$$\lambda_{w,\tau} \approx q^w f_\tau(w/\tau), \quad (\text{S31})$$

where $f_\tau(x)$ is defined by

$$\begin{aligned} f_\tau(x) &:= \int_0^x ds \sqrt{\frac{z_2 \tau}{2\pi(1-z_2)(1+s)}} \\ &\times \exp \left\{ \frac{[(1-z_2)s - z_2]^2}{2z_2(1-z_2)(1+s)} \tau \right\} \\ &= \int_0^{x\tau} dw' \sqrt{\frac{z_2}{2\pi(1-z_2)(w'+\tau)}} \\ &\times \exp \left\{ \frac{[(1-z_2)w' - z_2\tau]^2}{2z_2(1-z_2)(\tau+w')} \right\}. \end{aligned} \quad (\text{S32})$$

The approximation is numerically verified in Fig. S5 to be able to capture the leading singular value around the butterfly cone. It is noteworthy to mention that $f_\tau(x)$ is actually an integral of a Gaussian function along the LL direction. To see it, we transform the coordinates back to (x, t) though $x = w' - \tau$ and $t = w' + \tau$, and the integrand becomes

$$\begin{aligned} &\sqrt{\frac{z_2}{2\pi(1-z_2)t}} \exp \left\{ \frac{[x + (1-2z_2)t]^2}{8z_2(1-z_2)t} \right\} \\ &= \sqrt{\frac{z_2}{2\pi(1-z_2)}} \frac{1}{\sqrt{t}} \exp \left\{ \frac{[x + v_b t]^2}{2\sigma(t)^2} \right\} \end{aligned} \quad (\text{S33})$$

with $v_b = (q^2 - 1)/(q^2 + 1)$ and $\sigma(t) = 2q\sqrt{t}/(q^2 + 1)$. Here, we recover the butterfly velocity and the diffusion in this model by analyzing the behavior of the leading singular value.

VI. LIGHT-LIKE GENERATORS FOR TWO SPECIAL CASES

A. Dual unitary models

For DU circuits, we have $T_w |1^w\rangle = T_w^\dagger |1^w\rangle = |1^w\rangle$ and $T_w |0^w\rangle = T_w^\dagger |0^w\rangle = |0^w\rangle$, implying that the subspace spanned by $|1^w\rangle, |0^w\rangle$ is an invariant subspace of both T_w and T_w^\dagger . Hence, we only need to consider the restriction of the LLG on this subspace, and we have

$$T_w^\tau = \begin{bmatrix} 1 & \\ & 1 \end{bmatrix}, \quad F_w^\tau = \begin{bmatrix} 0 & -\sqrt{q^{2w}-1} \\ 0 & 1 \end{bmatrix}, \quad (\text{S34})$$

where we define $|0^w\rangle = [q^{w/2}, 0]^\top$ and $q^{w/2} |1^w\rangle = [1, \sqrt{q^{2w}-1}]^\top$. Hence, $\|F_w^\tau\| = q^w$.

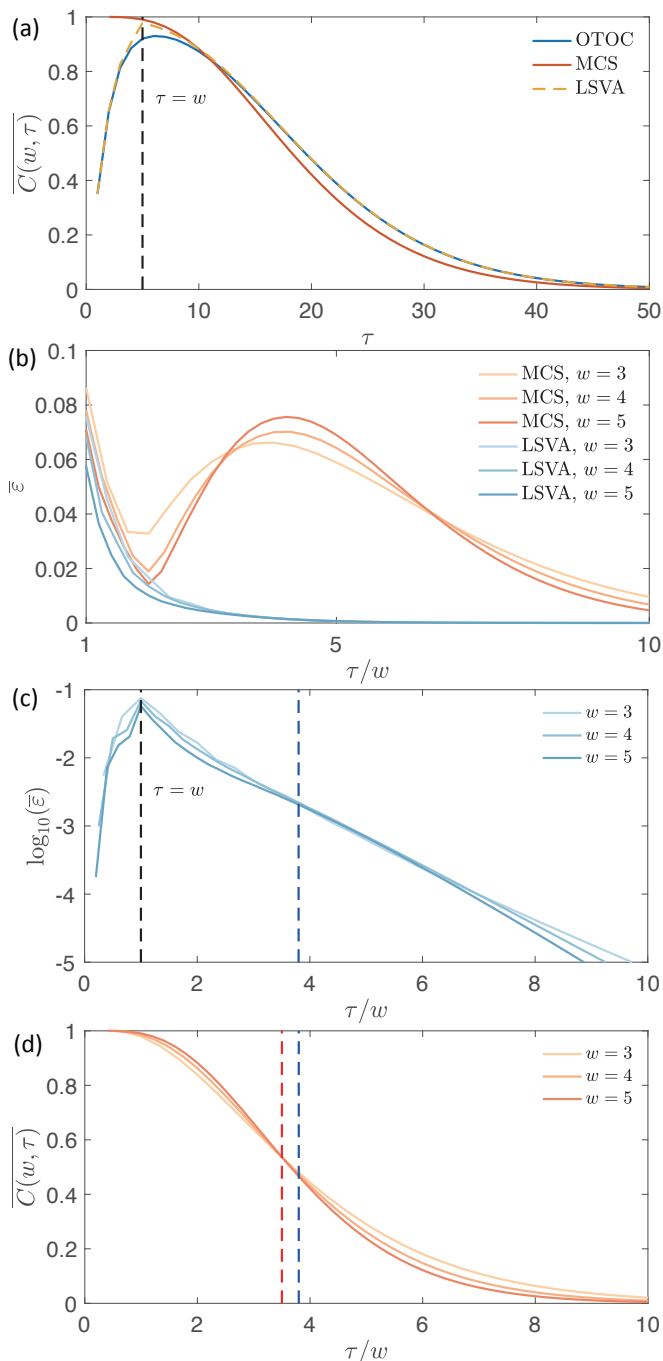


FIG. S6. (a) The value of OTOC, the OTOC projected on the MCS, and the LSVA of the spatial-temporal invariant 3PM with $w = 5$. Here, the results are averaged over the same 25 realizations as those in Fig. S9. (b) Ensemble average of the error $\epsilon = |C - C_{\text{MCS}}|$, and $\epsilon = |C - C_{\text{LSVA}}|$. (c) Error of the LSVA in the log scale. (d) OTOC projected on the MCS for different w . The red dashed line denotes the cross point of the OTOC projected on the MCS, and marks the effective butterfly velocity associated with this method. The blue dashed lines denote the position of corresponding butterfly velocity, v_b , at $\tau/w \approx 3.8$, which is extracted in an analogous figure for LSVA given by Fig. S9.

B. Completely localized models

If the two-site gate is a tensor product of two one-site gates, we then call the circuit a completely localized circuit. The LLGs of the completely localized circuits satisfy

$$\begin{aligned} T_w |0^m\rangle \otimes |1^n\rangle &= q |0^{m+1}\rangle \otimes |1^{n-1}\rangle, \\ T_w^\dagger |0^m\rangle \otimes |1^n\rangle &= q |0^{m-1}\rangle \otimes |1^{n+1}\rangle, \end{aligned} \quad (\text{S35})$$

where $m + n = w$ and $m, n > 0$. This implies $\|T_w\| \geq q$, which in conjunction with Eq. (S58) results in $\|T_w\| = q$. Moreover, the subspace spanned by all $|0^m\rangle \otimes |1^{w-m}\rangle$ with $m = 0, 1, \dots, w$ is an invariant subspace of both T_w and T_w^\dagger . Within this subspace, we particularly choose the following orthonormal basis, $|e_w\rangle = |0^w\rangle / q^{w/2}$ and for $m = 0, 1, \dots, w-1$

$$|e_m\rangle = |0^m\rangle \otimes \frac{q|1\rangle - |0\rangle}{q^{w/2}\sqrt{q^2-1}} \otimes |1^{w-m-1}\rangle. \quad (\text{S36})$$

Under this basis, for $\tau < w$, T_w^τ becomes

$$T_w^\tau = \begin{bmatrix} 0 & & & & & & & \\ \vdots & & & & & & & \\ 0 & & & & & & & \\ q^\tau & 0 & & & & & & \\ & & \ddots & & & & & \\ & & & q^\tau & & & & \\ & & & & 0 & \dots & 0 & \\ & & & & \chi(\tau) & \dots & \chi(1) & 1 \end{bmatrix}, \quad (\text{S37})$$

where $\chi(\tau) = q^{\tau-1}\sqrt{q^2-1}$. Because $q^{w/2}|1^w\rangle = [\chi(w), \chi(w-1), \dots, \chi(1), 1]^\top$, we obtain $\|F_w^\tau\| = q^w$ for $\tau < w$ and $\|F_w^\tau\| = 0$ for $\tau \geq w$.

VII. DIFFERENCE BETWEEN THIS WORK AND PERTURBATIVE RESULTS AROUND DU LIMIT IN [5]

Here we comment on the differences between the approach used in [5] and this paper. Consider the DU maximally chaotic subspace (MCS) defined as

$$\text{MCS} = \text{Span}\{|m, w-m\rangle = |0^m\rangle \otimes |1^{w-m}\rangle, \quad m = 0, 1, 2, \dots, w\}. \quad (\text{S38})$$

[5] approximated the OTOC by projecting the LLG onto the MCS for a model weakly perturbed from its dual unitarity (DU) limit, and derived (i) $v_b < v_{\text{LC}}$ [For DU circuits, it has been found that $v_b = v_{\text{LC}}$, see [6, 7]], and (ii) a diffusive front of the OTOC, coinciding with the one found in generic chaotic systems [8, 9].

In relation to this work, for the LLG projected onto the DU MCS in the weakly perturbed DU circuit, [5] showed that (i) the algebraic and geometric multiplicity of the subleading eigenvalue, z_2 , of the LLG projected onto the MCS is w and 1 respectively; and that (ii) the value of z_2 is independent of w . These latter two statements coincide with the statements in the

main text postulated and derived on z_2 in the generic chaotic case. However, we find that the projection of LLG onto the MCS of generic chaotic circuits does not capture OTOC in general, due to the following reasons:

1. **The MCS is generally not an approximately invariant subspace in spatial-temporal invariant generic chaotic circuits.** As the MCS is an exact invariant subspace for DU circuits, one might assume that it also works for weakly-perturbed DU circuits. However, the MCS is generally far from invariant in spatial-temporal invariant generic chaotic circuits. For example, this can be understood by considering LLGs of width $w = 1$. For the MCS to perform well, the subleading eigenvector of $T_{w=1}$ must be approximately in the MCS. However, the MCS of $w = 1$ is a 2-dimensional subspace of a q^4 -dimension Hilbert space, and the subleading eigenvector is generally far from such a small subspace. However, we numerically observe that the MCS works generically well in the averaged OTOC dynamics of spatial-temporal random circuits. We surmise that this is because the q^4 -dimension Hilbert space is reduced to a 2-dimensional subspace after ensemble averaging. Therefore, the MCS of $w = 1$ becomes the whole Hilbert space of $T_{w=1}$.
2. **Accuracy of OTOC calculated from LLG projected onto MCS decreases as w increases in spatial-temporal invariant generic chaotic circuits.** Numerically, we test the OTOC projected onto MCS in Fig. S6(a-c) for the spatial-temporal invariant 3PM. In Fig. S6(a), we find that there is a notable discrepancy between the OTOC and the projected OTOC. Furthermore, the accuracy of the projected OTOC decreases with increasing w , while the LSA performs better for increasing w as shown in Fig. S6(b) and S6(c).
3. **The value of the butterfly velocity v_b is not captured by the LLG projected onto MCS.** In Ref. [5], the error of the butterfly velocity comes from two approximations. The first one is the first-order perturbation that projects the LLG onto the MCS. The second one is the path integral method that treats the off-diagonal terms in the projected LLG perturbatively. In principle, the second error can be calculated order by order, and Ref. [5] obtained the analytical result up to the second order. However, the first error cannot be readily corrected by higher orders, and we numerically observe this error in Fig. S6(a) and S6(d).

The averaged OTOC dynamics of the spatial-temporal random HRM is exactly solvable [8, 9]. For such spatial-temporal random circuits, the OTOC can be written in terms of a (spatial-temporal invariant) LLG after performing the ensemble average in space and time. In VIII D, we derive the

eigenvalues, multiplicities, leading singular values, and the butterfly velocity associated to the LLG. As a side result from the analysis in VIII D, for the LLG of the averaged OTOC dynamics of the spatial-temporal random HRM, we derive that the MCS is an exact invariant subspace, and consequently, the LLG projected onto MCS can capture the OTOC in this model. However we expect that for generic spatial-temporal circuits, the MCS is not exactly invariant, because unlike DU circuits, in generic chaotic circuits, the invariance subspaces of the LLG, T_w , and its hermitian conjugate, T_w^\dagger , are generally not the same. We numerically verify that the MCS is not an exact invariant subspace for $w > 1$ in the spatial-temporal random RPM and 3PM (not at the DU limit).

VIII. MATHEMATICAL PROOFS

A. Proof of $|\sigma_{\text{spectrum}}(T_w)| \leq 1$

1. Large τ behaviour of T_w

In the main text, we show that the LLG T_w is generally not contracting, so one does not know a priori that its eigenvalues lie in the complex unit disk. Here, we provide proof that the eigenvalues indeed lie within the complex unit disk.

Let us first prove the following lemma: if the maximal modulus of the eigenvalue of a matrix T is $z_>$, then for two arbitrary sets of complete basis $\langle v_\alpha^L |$ and $| v_\beta^R \rangle$, then

$$\limsup_{\tau \rightarrow \infty} \frac{\left| \langle v_\alpha^L | T^\tau | v_\beta^R \rangle \right|}{\tau^{\varphi(z_>)} z_>^\tau} < +\infty, \quad (\text{S39})$$

and there exist a pair of basis vectors that makes this limit nonzero. Here, $\varphi(z)$ is determined by

$$\varphi(z) := \max_{i: |z_i|=|z|} \{N_i - 1\}, \quad (\text{S40})$$

where z_i and N_i are respectively the eigenvalue and the dimension of the i th Jordan block of T .

Suppose the Jordan normal form of T is given by

$$T = S^{-1} J S = S^{-1} \left[\sum_i (D_i + M_i) \right] S, \quad (\text{S41})$$

where D_i and M_i are the diagonal and off-diagonal parts of the i th Jordan block, respectively. As the basis is arbitrary, the invertible matrix can be absorbed into the basis, and thus, we set $T = J$ without loss of generality. Therefore, for $\tau > \varphi(z_>)$, we have

$$T^\tau = \sum_i \sum_{j=0}^{N_i-1} \binom{\tau}{j} (D_i)^{\tau-j} (M_i)^j. \quad (\text{S42})$$

Consequently, the limit becomes

$$\limsup_{\tau \rightarrow \infty} \frac{\left| \langle v_{\alpha}^L | T^{\tau} | v_{\beta}^R \rangle \right|}{\tau^{\varphi(z_{>})} z_{>}^{\tau}} = \limsup_{\tau \rightarrow \infty} \left| \sum_i \sum_{j=0}^{N_i-1} \frac{z_{>}^{-j}}{\tau^{\varphi(z_{>})}} \binom{\tau}{j} \left[\frac{z_i}{z_{>}} \right]^{\tau-j} \langle v_{\alpha}^L | [M_{z_i}]^j | v_{\beta}^R \rangle \right| = \limsup_{\tau \rightarrow \infty} \frac{\left| \langle v_{\alpha}^L | Q(\tau) | v_{\beta}^R \rangle \right|}{\varphi(z_{>})! z_{>}^{\varphi(z_{>})}}, \quad (\text{S43})$$

where $Q(\tau)$ denotes

$$Q(\tau) = \sum_{\substack{i: |z_i| = z_{>} \\ N_i = \varphi(z_{>}) + 1}} (z_i/z_{>})^{\tau - \varphi(z_{>})} (M_i)^{\varphi(z_{>})}. \quad (\text{S44})$$

Because $\|Q(\tau)\| = 1$ and all finite-dimensional norms are equivalent, we have that Eq. (S43) is always finite and

$$\limsup_{\tau \rightarrow \infty} \sum_{\alpha, \beta} \frac{\left| \langle v_{\alpha}^L | T^{\tau} | v_{\beta}^R \rangle \right|}{\tau^{\varphi(z_{>})} z_{>}^{\tau}} > 0, \quad (\text{S45})$$

meaning that the limit is nonzero for at least one pair of α, β .

2. Asymptotic behavior of the singular value

Note that ‘‘lim sup’’ can be replaced by ‘‘lim’’ if there is only one Jordan block contributing in Eq. (S44), because

$$\lim_{\tau \rightarrow \infty} \frac{\varphi(z_{>})! T^{\tau}}{\tau^{\varphi(z_{>})} z_{>}^{\tau - \varphi(z_{>})}} = (M_{z_{>}})^{\varphi(z_{>})} = |z_{>}^R\rangle \langle z_{>}^L|, \quad (\text{S46})$$

where $\langle z_{>}^L|, |z_{>}^R\rangle$ are the left and right eigenstates of eigenvalue $z_{>}$. What is more, we also have

$$\varphi(z_{>}) = a(z_{>}) - 1, \quad (\text{S47})$$

where $a(z)$ is the algebraic multiplicity of z . In this case, the singular value λ_{τ} is asymptotically given by

$$\lim_{\tau \rightarrow \infty} \frac{\varphi(z_{>})! \lambda_{\tau}}{\tau^{\varphi(z_{>})} z_{>}^{\tau - \varphi(\tau)} \left\| |z_{>}^R\rangle \right\| \left\| |z_{>}^L\rangle \right\|} = 1, \quad (\text{S48})$$

and the singular state satisfies

$$\lim_{\tau \rightarrow \infty} |\lambda_{\tau}^L\rangle = \frac{|z_{>}^R\rangle}{\|z_{>}^R\|}, \quad \lim_{\tau \rightarrow \infty} |\lambda_{\tau}^R\rangle = \frac{|z_{>}^L\rangle}{\|z_{>}^L\|}. \quad (\text{S49})$$

Applying the lemma to the LLG F_w , we expect that the OTOC should scale as $\tau^{\varphi[z_2(w), w]} z_2(w)^{\tau}$ at large τ , where $z_2(w)$ is the leading eigenvalue of F_w and equivalently, the subleading eigenvalue of T_w .

3. Proof of $\langle v_L | T_w^{\tau} | v_R \rangle < \infty$

Now, let us come back to the LLG. If the leading eigenvalue of T_w is greater than 1 and there are two sets of complete orthogonal basis, there exist two basis vectors satisfying

$$\limsup_{\tau \rightarrow \infty} |\langle v_L | T_w^{\tau} | v_R \rangle| = \infty. \quad (\text{S50})$$

Thus, there exists $\tau_0 > 0$ such that $|\langle v_L | T_w^{\tau_0} | v_R \rangle| > 1$.

On the other hand, by using σ_{α} ($\alpha = 1, 2, \dots, q^2$), one can construct a complete orthogonal basis with $\bigotimes_{i=1}^w [\sigma_{\alpha_i} \otimes_k \sigma_{\beta_i}]$. Here, the operator norm of the basis is normalized, $\|\sigma_{\alpha}\| = 1$. The desired pair of basis is thus given by

$$v_L = \frac{1}{q^{w/2}} \bigotimes_{i=1}^w \mathcal{T}_k [\sigma_{a_i} \otimes_k \sigma_{c_i}],$$

$$v_R = \frac{1}{q^{w/2}} \bigotimes_{i=1}^w [\sigma_{b_i} \otimes_k \sigma_{d_i}],$$

where \mathcal{T}_k represents the translation in the replicated space.

Next, we will prove that $|\langle v_L | T_w^{\tau_0} | v_R \rangle|$ must be equal or less than 1, resulting in the contradiction. Essentially, we will construct four operators A, B, C, D with $\|A\|, \|B\|, \|C\|, \|D\| \leq 1$, and an unitary evolution $U(t)$ that satisfying

$$\langle A(t) B C(t) D \rangle = \langle v_L | T_w^{\tau} | v_R \rangle, \quad (\text{S51})$$

where $A(t) = U(t)^{\dagger} A U(t)$ and $C(t) = U(t)^{\dagger} C U(t)$. If we find such construction, then we have

$$\begin{aligned} \langle v_L | T_w^{\tau} | v_R \rangle &= \langle A(t) B C(t) D \rangle \\ &\leq \|A(t) B C(t) D\| \\ &\leq \|A(t)\| \|B\| \|C(t)\| \|D\| \leq 1. \end{aligned} \quad (\text{S52})$$

Indeed, we can find such construction. A, C are given by

$$A = \mathbb{I}^{\tau} \otimes \bigotimes_{i=1}^w \sigma_{a_i}, \quad C = \mathbb{I}^{\tau} \otimes \bigotimes_{i=1}^w \sigma_{c_i}, \quad (\text{S53})$$

and they are supported on sites $x \in [\tau, w + \tau]$. B, D are given by

$$B = \bigotimes_{i=1}^w \sigma_{b_i} \otimes \mathbb{I}^{\tau}, \quad D = \bigotimes_{i=1}^l \sigma_{d_i} \otimes \mathbb{I}^{\tau}, \quad (\text{S54})$$

and they are supported on sites $x \in [1, w]$. For the evolution operator, we first define the evolution of each time step $\tilde{U}(t)$

$$\tilde{U}(t) = \mathbb{I}^{|t-\tau|} \otimes u^{w+\tau-|t-\tau|-|t-w|} \otimes \mathbb{I}^{|t-w|}. \quad (\text{S55})$$

The evolution operator is then defined as $U(t) = \prod_{t=1}^{w+\tau} \tilde{U}(t)$ as illustrated by Fig. S7. It is easy to verify that $\|A\|, \|B\|, \|C\|, \|D\| \leq 1$, and that Eq. (S51) is satisfied. This completes the proof.

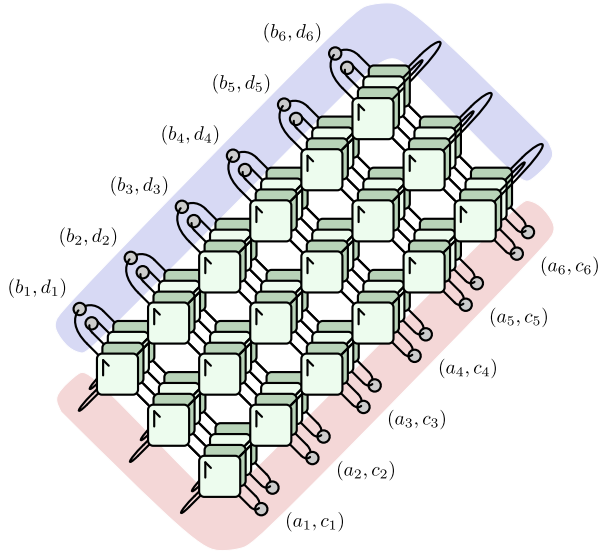


FIG. S7. An illustration for $\langle v_L | T_w^\tau | v_R \rangle$ with operators A and C highlighted in red, and B and D highlighted in blue.

4. Multiplicity of leading eigenvalues

From the construction, we also know that

$$\limsup_{\tau \rightarrow \infty} |\langle v_L | T_w^\tau | v_R \rangle| < \infty \quad (\text{S56})$$

is always finite. Hence, the modulus of the leading eigenvalue is less than or equal to 1. Moreover, the algebraic multiplicity of the eigenvalue with modulus 1 must equal the geometric multiplicity, or the OTOC grows algebraically.

B. Proof of $\|T_w\| \leq q$

Following from the construction in Section VIII A 3, we know that for an arbitrary vector $|v_R\rangle$, $T_w |v_R\rangle$ can be expressed as

$$\|T_w |v_R\rangle\| = \left\| P_r [\tilde{U} (\mathbb{I} \otimes v_R) \tilde{U}^\dagger] \right\|_F, \quad (\text{S57})$$

where $\|\cdot\|_F$ is the Frobenius norm, and $\tilde{U} = U \otimes_k U$ with U given by the construction. Here, we consider v_R as an operator acting on a Hilbert space of dimension q^{2w} , and $|0\rangle, |1\rangle$ correspond to the identity \mathbb{I} and the swap \mathbb{S} , respectively. Additionally, P_r is a projection operator that leaves only the component with the swap operator on the rightmost site, i.e. $\hat{O} \otimes \mathbb{S}$. Therefore, we have

$$\begin{aligned} \|T_w |v_R\rangle\| &\leq \left\| \tilde{U} (\mathbb{I} \otimes v_R) \tilde{U}^\dagger \right\|_F \\ &= \|\mathbb{I} \otimes v_R\|_F = \|\mathbb{I}\|_F \|v_R\|_F = q \|v_R\|, \end{aligned} \quad (\text{S58})$$

which completes the proof. This bound can be further improved to $\|T_w\| \leq 1$ for the dual-unitary case [4]. This means $\alpha \leq 1$, and the lower bound of α is trivial because the leading eigenvalue of T_w is 1.

On the other hand, the reducibility (see Fig. 1 in the main text) implies that a longer LLG inherits the spectrum of a shorter one. Furthermore, we can also conclude that $\|T_w\|$ increases monotonically with respect to w . Therefore, $\alpha = \lim_{w \rightarrow \infty} \ln(\|T_w\|) / \ln q$ exists.

C. Proof of $z_2(w) = z_2(w = 1)$

For the purpose of the proof, we introduce the generalized Pauli matrices, defined as

$$\sigma^{j,k} = \sum_{m=0}^{q-1} \omega^{jm} |m+k\rangle \langle m|, \quad (\text{S59})$$

where $j, k = 0, \dots, q-1$, and $\omega = e^{2\pi i/q}$. For convenience, we also use $\mu = j + qk$ to label $\sigma^{j,k}$. The generalized Pauli matrices satisfy $\text{tr}[(\sigma^\mu)^\dagger \sigma^\nu] = q \delta_{\mu\nu}$, and $\sigma^{j,k} \sigma^{j',k'} = \omega^{jk'} \sigma^{(j+j'),(k+k')}$. A useful identity is that for $\nu \neq 0$,

$$\sum_{\mu=1}^{q^2-1} \|[\sigma^\mu, \sigma^\nu]\|_F^2 = 2q^3. \quad (\text{S60})$$

What is more, we generalized OTOC for the generalized Pauli matrices, which are unitary but non-Hermitian,

$$\tilde{C}_{\mu\nu}(x, t) = 1 - \langle \sigma^\mu(0, t)^\dagger \sigma^\nu(x, 0)^\dagger \sigma^\mu(0, t) \sigma^\nu(x, 0) \rangle. \quad (\text{S61})$$

Hence, we have $C_{\mu\nu}(w, \tau) = \langle L_{\mu\nu} | F_w^\tau | R_{\mu\nu} \rangle$, where

$$\begin{aligned} \langle L_{\mu\nu} | &= \langle \mathbf{1}^{w-1} | \otimes_r \langle \mathbf{1}_{(\sigma^\nu)^\dagger, \sigma^\nu} |, \\ |R_{\mu\nu}\rangle &= |0_{(\sigma^\mu)^\dagger, \sigma^\mu}\rangle \otimes_r |0^{w-1}\rangle, \end{aligned} \quad (\text{S62})$$

and

$$\text{Re}[\tilde{C}_{\mu\nu}(x, t)] = \frac{1}{2} \langle [\sigma^\mu(0, t), \sigma^\nu(x, 0)]^\dagger [\sigma^\mu(0, t), \sigma^\nu(x, 0)] \rangle. \quad (\text{S63})$$

1. Main proof

Theorem 1. *If there exist μ and ν that*

$$\liminf_{\tau \rightarrow \infty} \frac{\text{Re}[C_{\mu\nu}(w, \tau)]}{\tau^{\varphi(w)} |z_2(w)|^\tau} > 0, \quad (\text{S64})$$

then $|z_2(w)| = |z_2(w-1)|$.

First, we have

$$\begin{aligned} \liminf_{\tau \rightarrow \infty} \frac{|C_{\mu\nu}(w, \tau)|}{\tau^{\varphi(w)} |z_2(w)|^\tau} &> 0, \\ \limsup_{\tau \rightarrow \infty} \frac{|C_{\mu\nu}(w, \tau)|}{\tau^{\varphi(w)} |z_2(w)|^\tau} &< \infty. \end{aligned} \quad (\text{S65})$$

Let P_2 be the projector operator of the 2-point correlation function part of the OTOC LLG, given by

$$P_2 = |\mathbb{I}^w\rangle\langle\mathbb{I}^w| \otimes_k \overline{|\mathbb{I}^w\rangle\langle\mathbb{I}^w|} + \overline{|\mathbb{I}^w\rangle\langle\mathbb{I}^w|} \otimes_k |\mathbb{I}^w\rangle\langle\mathbb{I}^w| \quad (\text{S66})$$

where the overline denotes the orthogonal complement of a projection operator. We have

$$P_2 |L\rangle = P_2 |R\rangle = 0, \quad F_w P_2 = P_2 F_w P_2. \quad (\text{S67})$$

We define $|R(\tau)\rangle = \bar{P}_2 F_w^\tau |R\rangle$, and have

$$\begin{aligned} X &= \limsup_{\tau \rightarrow \infty} \frac{\| |L\rangle \| |R(\tau)\rangle \|}{|\langle L | R(\tau) \rangle|} \\ &\leq \limsup_{\tau \rightarrow \infty} \frac{\| F_w^\tau \| |L\rangle \| |R\rangle \|}{|\langle L | R(\tau) \rangle|} < \infty. \end{aligned} \quad (\text{S68})$$

Further, we have

$$\begin{aligned} \langle L | R(\tau + N) \rangle &= \langle L | P_2 F_w^{\tau+N} |R\rangle \\ &= \langle L | F_w^N (P_2 + \bar{P}_2) F_w^\tau |R\rangle \\ &= \langle L | P_2 F_w^N P_2 F_w^\tau |R\rangle + \langle L | F_w^N \bar{P}_2 F_w^\tau |R\rangle \\ &= \langle L | F_w^N \bar{P}_2 F_w^\tau |R\rangle = \langle L | F_w^N |R(\tau)\rangle. \end{aligned} \quad (\text{S69})$$

We assume $|z_2(w)| > |z_2(w-1)|$ henceforth. By defining the projection operator $P_w = [|0^{w-1}\rangle\langle 0^{w-1}| / q^{w-1}] \otimes \mathbb{I}$, we can obtain

$$\limsup_{\tau \rightarrow \infty} \frac{\| |R(\tau)\rangle - |R'(\tau)\rangle \|}{\| |R(\tau)\rangle \|} = 0, \quad (\text{S70})$$

where $|R'(\tau)\rangle = P_w |R(\tau)\rangle = |0^{w-1}\rangle \otimes |\tilde{R}(\tau)\rangle$. The proof of this equation is left to the next section. Hence, we also have

$$\limsup_{\tau \rightarrow \infty} \frac{\| |R(\tau)\rangle - |R'(\tau)\rangle \|}{|\langle L | R(\tau) \rangle|} = 0, \quad (\text{S71})$$

Further, there is an integer N that $\| F_{w=1}^N \| < |z(w)|^N / (2X)$, because $\lim_{\tau \rightarrow \infty} \| F_{w=1}^\tau \|^{1/\tau} = |z_2(1)| < |z_2(w)|$.

For $\tau > N$, we have

$$\begin{aligned} \frac{|C_{\mu\nu}(w, \tau + N)|}{|C_{\mu\nu}(w, \tau)|} &\leq \frac{\| |L\rangle \| \| F_w^N \| \| |R(\tau)\rangle - |R'(\tau)\rangle \|}{|\langle L | R(\tau) \rangle|} \\ &\quad + \frac{|\langle L | F_w^N |R'(\tau)\rangle|}{|\langle L | R(\tau) \rangle|} \\ &\leq \frac{2^N q^{wN} \| |L\rangle \| \| |R(\tau)\rangle - |R'(\tau)\rangle \|}{|\langle L | R(\tau) \rangle|} \\ &\quad + \frac{|\langle \tilde{L} | F_1^N | \tilde{R}(\tau) \rangle|}{|\langle L | R(\tau) \rangle|} \\ &\leq 2^N q^{wN} \frac{\| |L\rangle \| \| |R(\tau)\rangle - |R'(\tau)\rangle \|}{|\langle L | R(\tau) \rangle|} \\ &\quad + \frac{|z_2(w)|^N \| |\tilde{L}\rangle \| \| |\tilde{R}(\tau)\rangle \|}{4X |\langle L | R(\tau) \rangle|} \end{aligned}$$

$$\begin{aligned} &\leq 2^N q^{wN} \frac{\| |L\rangle \| \| |R(\tau)\rangle - |R'(\tau)\rangle \|}{|\langle L | R(\tau) \rangle|} \\ &\quad + \frac{|z_2(w)|^N \| |L\rangle \| \| |R(\tau)\rangle \|}{2X |\langle L | R(\tau) \rangle|}. \end{aligned} \quad (\text{S72})$$

Here, we used $\| F_w \| \leq q^w + \| T_w \| \leq 2q^w$ for the second inequality. Therefore, we have

$$|z_2(w)|^N \leq \limsup_{\tau \rightarrow \infty} \frac{|C_{\mu\nu}(w, \tau + N)|}{|C_{\mu\nu}(w, \tau)|} \leq \frac{|z_2(w)|^N}{2}, \quad (\text{S73})$$

resulting in a contradiction.

Hence, if the premise is always satisfied, we obtain the following corollary,

Corollary 1.1. *If there exist μ_w and ν_w for all w that*

$$\liminf_{\tau \rightarrow \infty} \frac{\text{Re}[C_{\mu_w \nu_w}(w, \tau)]}{\tau^{\varphi(w)} |z_2(w)|^\tau} > 0, \quad (\text{S74})$$

then $z_2(w) = z_2(w-1)$.

2. Proof of Equation (S70)

From Eq. (S64) and assuming $|z_2(w)| > |z_2(w-1)|$, we know that

$$\lim_{\tau \rightarrow \infty} \frac{\sum_{w'=1}^{w-1} \sum_\alpha \text{Re}[C_{\mu\alpha}(w', \tau)]}{\sum_\alpha \text{Re}[C_{\mu\alpha}(w, \tau)]} = 0. \quad (\text{S75})$$

The evolution of the operator can be explicitly written as

$$\begin{aligned} \sigma^\mu(0, t) &= \sum'_{\alpha_1, \dots, \alpha_{w-1}} \sum_{\alpha_w} \sigma_{\alpha_1} \otimes \dots \otimes \sigma_{\alpha_w} \otimes A_{\alpha_1 \dots \alpha_w} \\ &\quad + \sum'_{\alpha_w} \mathbb{I}^{w-1} \otimes \sigma_{\alpha_w} \otimes A_{\alpha_w} \\ &\quad + \mathbb{I}^w \otimes A, \end{aligned} \quad (\text{S76})$$

where \sum' denotes that at least one index is nonzero. Using singular value decomposition, this can be reexpressed as

$$\sigma^\mu(0, t) = \sum_\gamma S_\gamma \otimes A'_\gamma + \sum_{\alpha=1}^{q^2-1} \mathbb{I}^{w-1} \otimes S_\alpha \otimes A'_\alpha + \mathbb{I}^w \otimes A, \quad (\text{S77})$$

where $S_\gamma, S_\alpha, A'_\gamma, A'_\alpha$ are orthogonal, and we adopt the following normalization $\| S_\alpha \|_{\text{F}}^2 = q$ and $\| S_\gamma \|_{\text{F}}^2 = q^w$. Hence, we have

$$\begin{aligned} q^\tau &= \sum'_{\alpha_1, \dots, \alpha_{w-1}} \sum_{\alpha_w} \| A_{\alpha_1 \dots \alpha_w} \|_{\text{F}}^2 + \sum_{\alpha_w} \| A_{\alpha_w} \|_{\text{F}}^2 + \| A \|_{\text{F}}^2 \\ &= \sum_\gamma \| A'_\gamma \|_{\text{F}}^2 + \sum_{\alpha=1}^{q^2-1} \| A'_\alpha \|_{\text{F}}^2 + \| A \|_{\text{F}}^2. \end{aligned} \quad (\text{S78})$$

Hence, we obtain the expansion for the OTOC with $w' < w$,

$$\sum_{\alpha} \text{Re}[C_{\mu\alpha}(w', \tau)] = \frac{q^2}{q^\tau} \sum_{\substack{\alpha_1, \dots, \alpha_w \\ \alpha_{w'} \neq 0}} \|A_{\alpha_1 \dots \alpha_w}\|_{\mathbb{F}}^2, \quad (\text{S79})$$

where we used Eq. (S60), and

$$\begin{aligned} \sum_{\alpha} \text{Re}[C_{\mu\alpha}(w, \tau)] &= \frac{q^2}{q^\tau} \sum'_{\alpha_1, \dots, \alpha_{w-1}} \sum'_{\alpha_w} \|A_{\alpha_1 \dots \alpha_w}\|_{\mathbb{F}}^2 \\ &+ \frac{q^2}{q^\tau} \sum'_{\alpha_w} \|A_{\alpha_w}\|_{\mathbb{F}}^2. \end{aligned} \quad (\text{S80})$$

Following this, we obtain

$$\sum_{w'=1}^{w-1} \sum_{\alpha} \text{Re}[C_{\mu\alpha}(w', \tau)] \geq \frac{q^2}{q^\tau} \sum'_{\alpha_1, \dots, \alpha_{w-1}} \sum_{\alpha_w} \|A_{\alpha_1 \dots \alpha_w}\|_{\mathbb{F}}^2, \quad (\text{S81})$$

and incorporating Eq. (S75), we deduce

$$\lim_{\tau \rightarrow \infty} \frac{\sum_{\gamma} \|A'_{\gamma}\|_{\mathbb{F}}^2}{\sum_{\alpha=1}^{q^2-1} \|A'_{\alpha}\|_{\mathbb{F}}^2} = 0. \quad (\text{S82})$$

Further, we know

$$\begin{aligned} q^{w/2} T_w^\tau |R\rangle &= \frac{1}{q^\tau} \text{tr}_{\tau}[\sigma^\mu(0, t)^\dagger \otimes_k \sigma^\mu(0, t)] \\ &= \frac{\|A\|_{\mathbb{F}}^2}{q^\tau} \mathbb{I}^w \otimes_k \mathbb{I}^w \\ &+ \mathbb{I}^w \otimes_k \mathbb{I}^{w-1} \otimes \sum_{\alpha=1}^{q^2-1} \frac{\text{tr}[A^\dagger A'_{\alpha}]}{q^\tau} S_{\alpha} \\ &+ \mathbb{I}^{w-1} \otimes \sum_{\alpha=1}^{q^2-1} \frac{\text{tr}[(A'_{\alpha})^\dagger A]}{q^\tau} S_{\alpha}^\dagger \otimes_k \mathbb{I}^w \\ &+ \mathbb{I}^w \otimes_k \sum_{\gamma} \frac{\text{tr}[A^\dagger A'_{\gamma}]}{q^\tau} S_{\gamma} + \sum_{\gamma} \frac{\text{tr}[(A'_{\gamma})^\dagger A]}{q^\tau} S_{\gamma}^\dagger \otimes_k \mathbb{I}^w \\ &+ \mathbb{I}^{w-1} \otimes \sum_{\alpha=1}^{q^2-1} \frac{\text{tr}[(A'_{\alpha})^\dagger A'_{\gamma}]}{q^\tau} S_{\alpha}^\dagger \otimes_k \sum_{\gamma} S_{\gamma} \\ &+ \sum_{\gamma} S_{\gamma}^\dagger \otimes_k \mathbb{I}^{w-1} \otimes \sum_{\alpha=1}^{q^2-1} \frac{\text{tr}[(A'_{\gamma})^\dagger A'_{\alpha}]}{2^\tau} S_{\alpha} \\ &+ \sum_{\alpha=1}^{q^2-1} \frac{\|A'_{\alpha}\|_{\mathbb{F}}^2}{q^\tau} S_{\alpha}^\dagger \otimes S_{\alpha} + \sum_{\gamma} \frac{\|A'_{\gamma}\|_{\mathbb{F}}^2}{q^\tau} S_{\gamma}^\dagger \otimes S_{\gamma}. \end{aligned} \quad (\text{S83})$$

Hence,

$$\begin{aligned} &q^{w/2} |R(\tau)\rangle \\ &= q^{w/2} \bar{P}_2 T_w^\tau |R\rangle - q^{w/2} |0^w\rangle \\ &= - \left(\sum_{\gamma} \|A'_{\gamma}\|_{\mathbb{F}}^2 + \sum_{\alpha=1}^{q^2-1} \|A'_{\alpha}\|_{\mathbb{F}}^2 \right) \mathbb{I}^w \otimes_k \mathbb{I}^w \end{aligned}$$

$$\begin{aligned} &+ \mathbb{I}^{w-1} \otimes \sum_{\alpha=1}^{q^2-1} \frac{\text{tr}[(A'_{\alpha})^\dagger A'_{\gamma}]}{q^\tau} S_{\alpha}^\dagger \otimes_k \sum_{\gamma} S_{\gamma} \\ &+ \sum_{\gamma} S_{\gamma}^\dagger \otimes_k \mathbb{I}^{w-1} \otimes \sum_{\alpha=1}^{q^2-1} \frac{\text{tr}[(A'_{\gamma})^\dagger A'_{\alpha}]}{2^\tau} S_{\alpha} \\ &+ q^{w/2} |0^w\rangle \otimes \sum_{\alpha=1}^{q^2-1} \frac{\|A'_{\alpha}\|_{\mathbb{F}}^2}{q^\tau} S_{\alpha}^\dagger \otimes_k S_{\alpha} + \sum_{\gamma} \frac{\|A'_{\gamma}\|_{\mathbb{F}}^2}{q^\tau} S_{\gamma}^\dagger \otimes_k S_{\gamma}. \end{aligned} \quad (\text{S84})$$

We do the following decomposition,

$$|R(\tau)\rangle = |R_*(\tau)\rangle + |R'(\tau)\rangle. \quad (\text{S85})$$

The norm of the two terms can be estimated by

$$\frac{\langle R'(\tau) | R'(\tau) \rangle}{q^{w-2\tau}} \geq \sum_{\alpha=1}^{q^2-1} \|A'_{\alpha}\|_{\mathbb{F}}^4 \geq \frac{1}{q^2-1} \left[\sum_{\alpha=1}^{q^2-1} \|A'_{\alpha}\|_{\mathbb{F}}^2 \right]^2 \quad (\text{S86})$$

and

$$\begin{aligned} &\frac{\langle R_*(\tau) | R_*(\tau) \rangle}{q^{w-2\tau}} \\ &= 2 \sum_{\alpha=1}^{q^2-1} \sum_{\gamma} |\text{tr}[(A'_{\alpha})^\dagger A'_{\gamma}]|^2 + \sum_{\gamma} \|A'_{\gamma}\|_{\mathbb{F}}^4 \\ &\leq 2 \sum_{\alpha=1}^{q^2-1} \sum_{\gamma} \|A'_{\alpha}\|_{\mathbb{F}}^2 \|A'_{\gamma}\|_{\mathbb{F}}^2 + \left[\sum_{\gamma} \|A'_{\gamma}\|_{\mathbb{F}}^2 \right]^2 \\ &= 2 \left[\sum_{\alpha=1}^{q^2-1} \|A'_{\alpha}\|_{\mathbb{F}}^2 \right] \left[\sum_{\gamma} \|A'_{\gamma}\|_{\mathbb{F}}^2 \right] + \left[\sum_{\gamma} \|A'_{\gamma}\|_{\mathbb{F}}^2 \right]^2. \end{aligned} \quad (\text{S87})$$

This implies that

$$\lim_{\tau \rightarrow \infty} \frac{\| |R_*(\tau)\rangle \|}{\| |R'(\tau)\rangle \|} = 0, \quad (\text{S88})$$

and thus,

$$\lim_{\tau \rightarrow \infty} \frac{\| |R(\tau)\rangle - |R'(\tau)\rangle \|}{\| |R(\tau)\rangle \|} = 0, \quad (\text{S89})$$

D. Spatial-temporal random Haar-random model

In this section, we will analytically solve the eigenvalues of the ensemble-averaged LLG for the spatial-temporal random HRM. Essentially, we adopt a particular similar transformation that makes the LLG an upper-triangular matrix, and consequently, the eigenvalues are given by the diagonal entries.

1. Similar transformation

Note that the basis is not orthogonal here, and it satisfies

$$\langle i|j\rangle = q\delta_{ij} + \delta_{i\bar{j}}, \quad (\text{S90})$$

where $\bar{i} = 1 - i$. To simplify the proof, we convert Eq. (S28) into the biorthogonal basis,

$$\bar{\mathcal{U}}_2 = M_{j_1 j_2}^{i_1 i_2} |i_1\rangle |j_1'\rangle \langle i_2| \langle j_2'|, \quad (\text{S91})$$

where $|i'\rangle$ is defined by $\langle i|j'\rangle = \delta_{ij}$. Hence, we have $|i\rangle = U_i^j |j'\rangle$ with $U_i^j = q\delta_i^j + \delta_i^{\bar{j}}$, and

$$M_{j_1 j_2}^{i_1 i_2} = U_{j_1}^k U_{j_2}^l \delta^{i_1 i_2} q^2 \text{Wg}(i_1^{-1} k, q^2). \quad (\text{S92})$$

If $j_1 = j_2 = i_1$, we have

$$M_{00}^{00} = q^2 q^2 \frac{1}{q^4 - 1} - q^2 \frac{1}{q^2(q^4 - 1)} = 1. \quad (\text{S93})$$

If $j_1 \neq j_2$, we have

$$M_{01}^{00} = q^3 \frac{1}{q^4 - 1} - q^3 \frac{1}{q^2(q^4 - 1)} = \frac{q}{q^2 + 1}. \quad (\text{S94})$$

To summarise, the nonvanishing entries of \tilde{M} are

$$M_{01}^{00} = M_{10}^{00} = M_{01}^{11} = M_{01}^{11} = \frac{q}{q^2 + 1}, \quad (\text{S95})$$

$$M_{00}^{00} = M_{11}^{11} = 1. \quad (\text{S96})$$

Obviously, M satisfies the following symmetry

$$M_{ij}^{kl} = M_{\bar{i}\bar{j}}^{\bar{k}\bar{l}}. \quad (\text{S97})$$

The light-like (LL) generator is given by

$$\begin{aligned} T_{(j_1 j_2 \dots j_w)}^{(i_1 i_2 \dots i_w)} &= M_{0j_1}^{i_1 \mu_1} M_{\mu_1 j_2}^{i_2 \mu_2} \dots M_{\mu_{w-1} j_w}^{i_w \alpha} (\alpha|1) \\ &= M_{0j_1}^{i_1 \mu_1} M_{\mu_1 j_2}^{i_2 \mu_2} \dots M_{\mu_{w-1} j_w}^{i_w 0} \\ &\quad + q M_{0j_1}^{i_1 \mu_1} M_{\mu_1 j_2}^{i_2 \mu_2} \dots M_{\mu_{w-1} j_w}^{i_w 1}. \end{aligned} \quad (\text{S98})$$

Thus, the LLG contains two terms for $\alpha = 0$ and $\alpha = 1$. Moreover, because of Eq. (S95), the tensor contraction can be reduced to a simple product,

$$M_{0j_1}^{i_1 \mu_1} M_{\mu_1 j_2}^{i_2 \mu_2} \dots M_{\mu_{w-1} j_w}^{i_w \alpha} = M_{0j_1}^{i_1 i_1} \times M_{i_1 j_2}^{i_2 i_2} \times \dots \times M_{i_{w-1} j_w}^{i_w \alpha}, \quad (\text{S99})$$

where the right-hand side has no Einstein summation.

The next step is to reorder the basis so that the LLG becomes upper triangular. Before the proof, it is useful to introduce three propositions of the LLG.

Proposition 1. $T_{(0j_2 \dots j_w)}^{(i_2 \dots i_w)} = 0$.

This is because $M_{00}^{11} = 0$ according to Eq. (S95).

Proposition 2. $T_{(0j_2 \dots j_w)}^{(0i_2 \dots i_w)} = T_{(j_2 \dots j_w)}^{(i_2 \dots i_w)}$.

This is because $M_{00}^{00} = 1$ according to Eq. (S95).

Proposition 3. If $T_{(0j_2 \dots j_w)}^{(0i_2 \dots i_w)} = 0$, then $T_{(1\bar{j}_2 \dots \bar{j}_w)}^{(1\bar{i}_2 \dots \bar{i}_w)} = 0$.

First, we have $T_{(0j_2 \dots j_w)}^{(0i_2 \dots i_w)} = T_{(j_2 \dots j_w)}^{(i_2 \dots i_w)} = 0$. As two terms in Eq. (S98) are nonnegative, $T_{(j_2 \dots j_w)}^{(i_2 \dots i_w)} = 0$ implies that

$$\begin{aligned} M_{0j_2}^{i_2 i_2} \times \dots \times M_{i_{w-1} j_w}^{i_w 0} \\ = M_{0j_1}^{i_1 i_1} \times M_{0j_2}^{i_2 i_2} \times \dots \times M_{i_{w-1} j_w}^{i_w 1} = 0. \end{aligned} \quad (\text{S100})$$

Further, because of the symmetry given in Eq. (S97), we obtain

$$\begin{aligned} M_{01}^{11} \times M_{1\bar{j}_2}^{\bar{i}_2 \bar{i}_2} \times \dots \times M_{i_{w-1} \bar{j}_w}^{\bar{i}_w 1} \\ = M_{01}^{11} \times M_{1\bar{j}_1}^{\bar{i}_1 \bar{i}_1} \times M_{1\bar{j}_2}^{\bar{i}_2 \bar{i}_2} \times \dots \times M_{i_{w-1} \bar{j}_w}^{\bar{i}_w 0} = 0. \end{aligned} \quad (\text{S101})$$

Therefore, we have $T_{(1\bar{j}_2 \dots \bar{j}_w)}^{(1\bar{i}_2 \dots \bar{i}_w)} = 0$.

Using these three propositions, we can construct a map $\sigma_w(m) = (i_1 i_2 \dots i_w)$ where $m = 0, \dots, 2^w - 1$, satisfying $T_{\sigma_w(n)}^{\sigma_w(m)} = 0$ if $m > n$. We will do this by induction. For $w = 1$, let

$$\sigma_1(0) = 0, \quad \sigma_1(1) = 0, \quad (\text{S102})$$

and then $T_{(0)}^{(1)} = 0$ because of Prop. 1. Supposing that we have such a map for $w - 1$, then for w , we define

$$\begin{aligned} \sigma_w(m) &= (0 \sigma_{w-1}(m)), \\ \sigma_w(2^{w-1} + m) &= \left(1 \overline{\sigma_{w-1}(m)}\right), \end{aligned} \quad (\text{S103})$$

for $m = 0, 1, \dots, 2^{w-1} - 1$.

If $2^{w-1} > m > n$, then $T_{\sigma_w(n)}^{\sigma_w(m)} = T_{(0 \sigma_{w-1}(n))}^{(0 \sigma_{w-1}(m))} = 0$ because of Prop. 2.

If $m + 2^{w-1} \geq 2^{w-1} > n$, then $T_{\sigma_w(n)}^{\sigma_w(m+2^{w-1})} = T_{(0 \sigma_{w-1}(n))}^{(1 \overline{\sigma_{w-1}(m)})} = 0$ because of Prop. 1.

If $m + 2^{w-1} > n + 2^{w-1} \geq 2^{w-1}$, then $T_{\sigma_w(n+2^{w-1})}^{\sigma_w(m+2^{w-1})} = T_{(1 \overline{\sigma_{w-1}(n)})}^{(1 \overline{\sigma_{w-1}(m)})} = 0$ because of Prop. 3.

Hence, the construction of $\sigma_w(m)$ is legitimate.

2. Eigenvalues

We have proved that $T_{(j_1 j_2 \dots j_w)}^{(i_1 i_2 \dots i_w)}$ is upper-triangular before reordering, and thus, the eigenvalues are given by $T_{(i_1 i_2 \dots i_w)}^{(i_1 i_2 \dots i_w)}$ for all $(i_1 i_2 \dots i_w)$. That is, we need to evaluate

$$\begin{aligned} T_{(i_1 i_2 \dots i_w)}^{(i_1 i_2 \dots i_w)} &= M_{0i_1}^{i_1 i_1} M_{i_1 i_2}^{i_2 i_2} \dots M_{i_{w-1} 0}^{i_w 0} \delta_{i_w, 0} \\ &\quad + q M_{0i_1}^{i_1 i_1} M_{i_1 i_2}^{i_2 i_2} \dots M_{i_{w-1} 1}^{i_w 1} \delta_{i_w, 1}. \end{aligned} \quad (\text{S104})$$

Each $M_{i_{k-1} i_k}^{i_k i_k}$ contributes $\frac{q}{q^2 + 1}$ if $i_{k-1} \neq i_k$, or 1 if $i_{k-1} = i_k$. What is more, i_w contributes 1 for $i_w = 0$, and q for $i_w =$

1. Therefore, it amounts to counting the number of domain walls in $0i_1i_2 \cdots i_{w-1}0$ (PBC) and $0i_1i_2 \cdots i_{w-1}1$ (twisted PBC). Here, we regard the length of these two chains as w .

It is readily to prove that PBC only has even numbers of domain walls, and that twisted PBC only has odd numbers. Further, we have the following recursive relation

$$\begin{aligned} f_{\text{PBC}}(w, n) &= f_{\text{PBC}}(w-1, n) + f_{\text{IPBC}}(w-1, n-1), \\ f_{\text{IPBC}}(w, n) &= f_{\text{IPBC}}(w-1, n) + f_{\text{PBC}}(w-1, n-1), \end{aligned} \quad (\text{S105})$$

where $f_{\text{PBC/IPBC}}(w, n)$ is the number of states with n domain walls in a chain of length w . Using induction, one can prove that $f_{\text{PBC/IPBC}}(w, n) = \binom{w}{n}$ for even or odd n respectively.

In conclusion, the eigenvalues of the LLG are

$$\varepsilon_n = \begin{cases} \left(\frac{q}{q^2+1}\right)^n & n \text{ even,} \\ q \left(\frac{q}{q^2+1}\right)^n & n \text{ odd,} \end{cases} \quad (\text{S106})$$

with algebraic multiplicity $\binom{w}{n}$. Here, n takes value from $0, 1, \dots, w-1$.

3. Geometric multiplicity of the subleading eigenvalue

From the previous section, the subleading eigenvalue is $q^2/(q^2+1)$ with algebraic multiplicity w . In this section, we will prove that its geometric multiplicity is one. Considering the subspace V_w spanned by all $|0^m\rangle \otimes |1^{w-m}\rangle$ with $m = 0, 1, \dots, w$ is an invariant subspace of both T_w and T_w^\dagger . Within this subspace, we particularly choose the following orthonormal basis, $|e_w\rangle = |0^w\rangle/q^{w/2}$ and for $m = 0, 1, \dots, w-1$. It is easy to prove that $T_w|1^w\rangle \in V_w$ using induction. To see it, supposing $T_w|1^w\rangle \in V_w$, we have for $|1^{w+1}\rangle$,

$$\begin{aligned} &\frac{q^2+1}{q} T_{w+1} |1^{w+1}\rangle \\ &= |0\rangle \otimes T_w |1^w\rangle + |1\rangle \otimes (1 | \bigcirc_r \overline{U}_2 |1\rangle |1^w\rangle \\ &= |0\rangle \otimes T_w |1^w\rangle + |1^{w+1}\rangle. \end{aligned} \quad (\text{S107})$$

As $|0\rangle \otimes T_w |1^w\rangle$ and $|1^{w+1}\rangle$ belong to V_{w+1} , we have $T_{w+1} |1^{w+1}\rangle \in V_{w+1}$. Further, $T_w |1^w\rangle \in V_w$ implies $T_{w+m} |0^m\rangle \otimes |1^w\rangle \in V_{w+m}$ because of the reducibility, and thus, V_w is an invariant subspace of both T_w and T_w^\dagger . Within this subspace, we choose the following orthonormal basis, $|e_w\rangle = |0^w\rangle/q^{w/2}$ and for $m = 0, 1, \dots, w-1$

$$|e_m\rangle = |0^m\rangle \otimes \frac{|v\rangle}{q^{w/2}\sqrt{q^2-1}} \otimes |1^{w-m-1}\rangle, \quad (\text{S108})$$

where $|v\rangle = q|1\rangle - |0\rangle$. Note that in this basis, the $|1\rangle$ is given by

$$q^{w/2} |1^w\rangle = [\chi(w), \chi(w-1), \dots, \chi(1), 1]^\top, \quad (\text{S109})$$

where $\chi(j) = q^{j-1}\sqrt{q^2-1}$. Because $\langle 0|v\rangle = 0$, we have $\langle e_m|T_w|e_n\rangle = 0$ if $m < n$, meaning that T_w is lower-triangular in this basis. By direct calculation, we also have $\langle e_w|T_w|e_w\rangle = 1$, $\langle e_m|T_w|e_m\rangle = q^2/(q^2+1)$ for $m \leq w-1$, and $\langle e_{m+1}|T_w|e_m\rangle = q^3/(q^2+1)^2$ for $m \leq w-2$. Hence, the subspace contains all the Jordan blocks (if there are more than one) of the subleading eigenvalue. What is more, as the $\langle e_{m+1}|T_w|e_m\rangle \neq 0$ for $m \leq w-2$ means that the geometric multiplicity of the subleading eigenvalue is one. This is because if there is more than one eigenvector, then there must be an eigenvector $|\psi\rangle$ that $\langle e_m|\psi\rangle$ for some $m \leq w-2$. Suppose that $m_0 \leq w-2$ is the smallest one among such m -s, and that $\langle m_0|\psi\rangle = 1$. We then have

$$\begin{aligned} &\frac{q^2}{q^2+1} \langle e_{m_0+1}|\psi\rangle = \langle e_{m_0+1}|T_w|\psi\rangle \\ &= \langle e_{m_0+1}|T_w|e_{m_0}\rangle + \frac{q^2}{q^2+1} \langle e_{m_0+1}|\psi\rangle, \end{aligned} \quad (\text{S110})$$

leading to $\langle e_{m_0+1}|T_w|e_{m_0}\rangle = 0$. Therefore, we prove that the temporal-spatial random HRM follows the two conjectures in the main text.

4. Leading singular value around the butterfly cone

Because $|1^w\rangle, |0^w\rangle$, and the subleading generalized eigenstates all belong to V_w , it is reasonable to assume that the leading singular states reside in this subspace. Thus, we only consider the LLG in this subspace in this section. The restriction of T_w to V_w can be calculated exactly. Because

$$\begin{aligned} T_{w=1}^\dagger |v\rangle &= \frac{q^2|v\rangle}{q^2+1} \\ \langle v| \langle 0|\overline{U}_2 |v\rangle &= \frac{q|v\rangle}{q^2+1}, \end{aligned} \quad (\text{S111})$$

we have for $n \geq 1$ and $m \leq w-2$

$$\begin{aligned} \langle e_{m+n}|T_w|e_m\rangle &= \left(\frac{q}{q^2+1}\right)^{n-1} \langle e_{m+1}|T_w|e_m\rangle \\ &= \left(\frac{q}{q^2+1}\right)^n \frac{q^2}{q^2+1}. \end{aligned} \quad (\text{S112})$$

Hence, T_w in subspace V_w can be expressed as

$$T'_w = \begin{bmatrix} z_2 & & & & & & \\ z_2(z_2/q) & z_2 & & & & & \\ z_2(z_2/q)^2 & z_2(z_2/q) & z_2 & & & & \\ \vdots & \ddots & \ddots & \ddots & & & \\ z_2(z_2/q)^{w-1} & \cdots & z_2(z_2/q)^2 & z_2(z_2/q) & z_2 & & \\ y_w & \cdots & y_3 & y_2 & y_1 & 1 & \end{bmatrix}, \quad (\text{S113})$$

where $z_2 = q^2/(q^2+1)$, and y_i are some coefficients to be determined. The matrix can be simplified to

$$T'_w = \begin{bmatrix} R & 0 \\ y & 1 \end{bmatrix}, \quad (\text{S114})$$

where $y = (y_w, y_{w-1}, \dots, y_1)$, $R = [(1 + q^{-2}) - M/q]^{-1}$ and

$$M = \begin{bmatrix} 0 & & & & & \\ 1 & 0 & & & & \\ 0 & 1 & 0 & & & \\ \vdots & \ddots & \ddots & \ddots & & \\ 0 & \dots & 0 & 1 & 0 & \end{bmatrix}. \quad (\text{S115})$$

As $\langle 1^w | \propto [\chi, 1] := [\chi(w), \chi(w-1), \dots, \chi(1), 1]$ is a left eigenstate of T_w , we then have

$$[\chi, 1] = [\chi, 1]T'_w = [\chi R + y, 1], \quad (\text{S116})$$

meaning that $y = \chi - \chi R$. Therefore, we obtain

$$F'_w = \begin{bmatrix} R & 0 \\ -\chi R & 0 \end{bmatrix}, \quad (\text{S117})$$

and

$$(F'_w)^\tau = \begin{bmatrix} R^\tau & 0 \\ -\chi R^\tau & 0 \end{bmatrix}. \quad (\text{S118})$$

The leading singular value $\lambda_{w,\tau}$ is the square root of leading eigenvalue of

$$(F'_w)^\tau (F'_w)^\tau = (R^\dagger)^\tau R^\tau + (R^\dagger)^\tau \chi \chi^\dagger R^\tau. \quad (\text{S119})$$

As $\|\chi\| = \sqrt{q^{2w} - 1}$, the leading eigenvalue of $(F'_w)^\tau (F'_w)^\tau$ is dominated by the second term, and correspondingly, $\lambda_{w,\tau} \approx \|\chi R^\tau\|$. Further, R^τ can be calculated from Taylor expansion,

$$R^\tau = \left(\frac{q^2}{q^2 + 1}\right)^\tau \sum_{k=0}^{w-1} \binom{\tau + k - 1}{k} \left(\frac{q}{q^2 + 1}\right)^k M^k, \quad (\text{S120})$$

where we use the identity $M^w = 0$. The j th component of χR^τ is given by

$$\begin{aligned} [\chi R^\tau]_j &= \left(\frac{q^2}{q^2 + 1}\right)^\tau \sum_{k=0}^j \binom{\tau + k - 1}{k} \left(\frac{q}{q^2 + 1}\right)^k \\ &\quad \times \chi(w - k - j) \\ &= \chi(w - j) \sum_{k=0}^j \binom{\tau + k - 1}{k} (1 - z_2)^k z_2^\tau. \end{aligned} \quad (\text{S121})$$

Note that $\sum_{k=0}^{\infty} \binom{\tau + k - 1}{k} (1 - z_2)^k = z_2^{-\tau}$, so $[\chi R^\tau]_j \leq [\chi]_j$. For large τ and $j/\tau \approx q^2$, using Stirling's formula, we have

$$\begin{aligned} [\chi R^\tau]_j &\approx \chi(w - j) \sum_{w'=0}^j \sqrt{\frac{z_2}{2\pi(1 - z_2)(\tau + w' - 1)}} \\ &\quad \times \exp\left\{\frac{[(1 - z_2)w' - z_2(\tau - 1)]^2}{2z_2(1 - z_2)(w' + \tau - 1)}\right\} \\ &\approx \chi(w - j) f_\tau(j/\tau), \end{aligned} \quad (\text{S122})$$

where $f_\tau(x)$ is defined by

$$\begin{aligned} f_\tau(x) &:= \int_0^x ds \sqrt{\frac{z_2^\tau}{2\pi(1 - z_2)(1 + s)}} \\ &\quad \times \exp\left\{\frac{[(1 - z_2)s - z_2]^2}{2z_2(1 - z_2)(1 + s)}\right\} \\ &= \int_0^{x\tau} dw' \sqrt{\frac{z_2}{2\pi(1 - z_2)(w' + \tau)}} \\ &\quad \times \exp\left\{\frac{[(1 - z_2)w' - z_2\tau]^2}{2z_2(1 - z_2)(\tau + w')}\right\}. \end{aligned} \quad (\text{S123})$$

As $\|\chi R^\tau\|$ is dominated by components with $j/w \approx 1$, we obtain

$$\|\chi R^\tau\| \approx \|\chi\| f_\tau(w/\tau) \approx q^w f_\tau(w/\tau). \quad (\text{S124})$$

IX. ADDITIONAL NUMERICS

In this section, we provide additional numerics for the behavior of the OTOC around the butterfly cone, the performance of the LSVA and the variation method, and the w -dependence of the large τ behavior in various models.

A. OTOC, LSVA, and the variation method in the spatial-temporal invariant models

In this subsection, we provide: (i) The OTOC and the error of LSVA in the XYZc model in Fig. S8, (ii) the sharpening of the OTOC around the butterfly cone in the 3PM in Fig. S9, (iii) overlap between the leading singular states and the variational states in the 3PM in Fig. S10.

B. OTOC, LSVA, and the variation method in the spatial-temporal random HRM

In this subsection, we provide: (i) Comparison between OTOC, LSVA and variational method in this model in Fig. S11, (ii) the sharpening of the OTOC around the butterfly cone and the error of LSVA in this model in Fig. S12.

C. w -dependence of the large τ behavior

In this subsection, we provide the large τ behavior for different w in various models in Fig. S13.

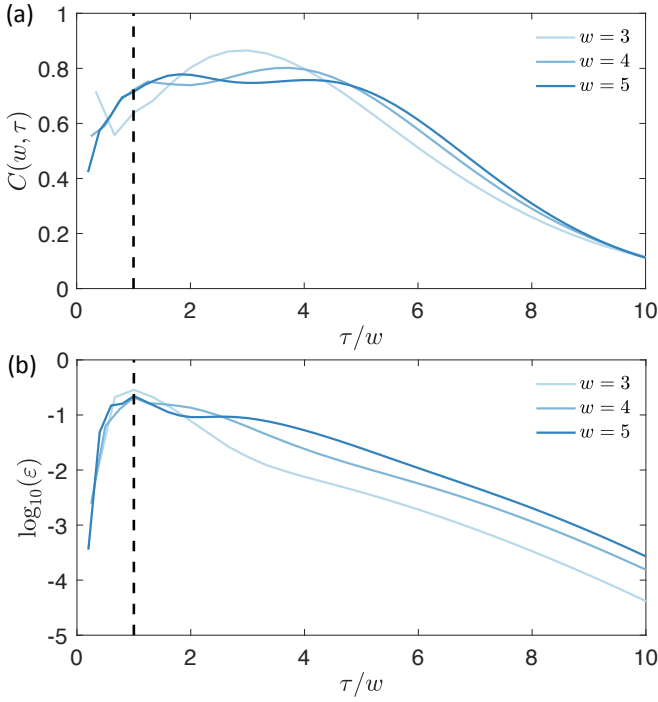


FIG. S8. (a) OTOC around the butterfly cone and (b) error $\epsilon = |C - C_{\text{LSVA}}|$ in the spatial-temporal invariant XYZc model. The black dashed lines denote $\tau/w = 1$, and we use the same parameters as those in the main text.

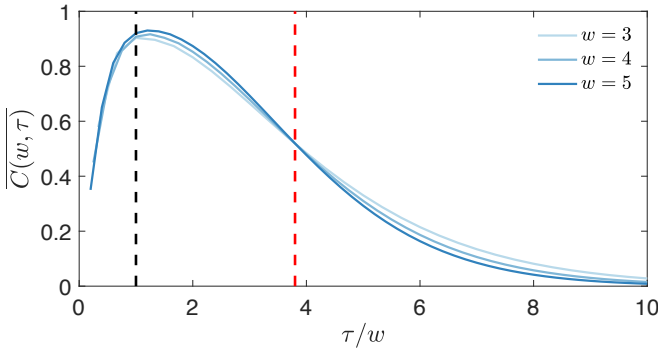


FIG. S9. (a) Ensemble-averaged OTOC around the butterfly cone in the spatial-temporal invariant 3PM. The black dashed lines denote $\tau/w = 1$, and the red ones denote the crossing point of the OTOC at $\tau/w = 3.8$. Here, the results are averaged over 25 realizations.

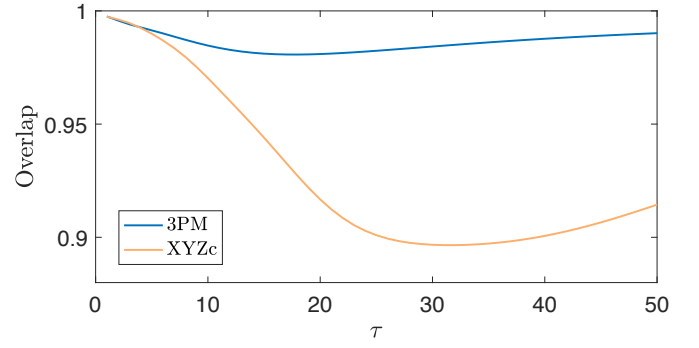


FIG. S10. Overlap between the exact leading singular state of the left-moving LLG and the variational ansatz, defined by $|\langle \lambda_{w,\tau}^{\text{L,VP}} | \lambda_{w,\tau}^{\text{L}} \rangle \langle \lambda_{w,\tau}^{\text{R}} | \lambda_{w,\tau}^{\text{R,VP}} \rangle|$. Here, we calculate the spatial-temporal invariant case with $w = 5$, and use the same realization as that in the main text.

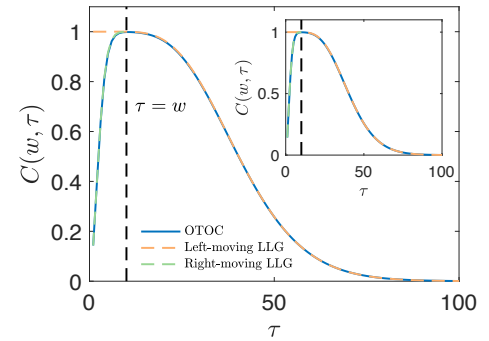


FIG. S11. OTOC of the spatial-temporal random HRM with $q = 2$ and $w = 10$. The dashed lines in the main panel and the inset represent the LSVA and the variational method, respectively.

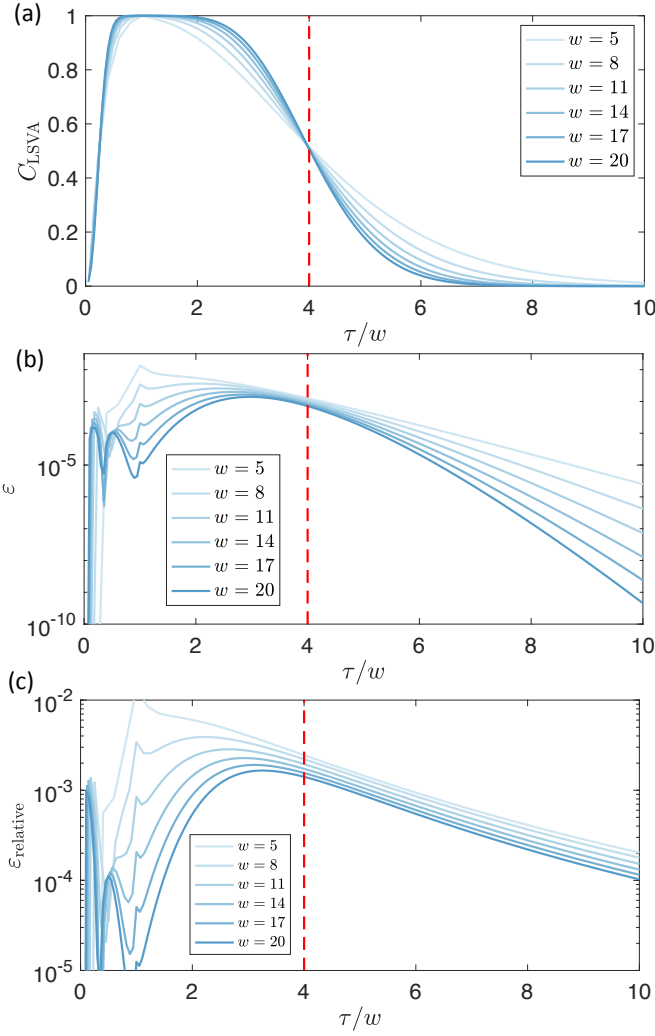


FIG. S12. (a) LSVAs around the butterfly cone, (b) error $\varepsilon = |C - C_{\text{LSVA}}|$, and (c) relative error $\varepsilon_{\text{relative}} = |C - C_{\text{LSVA}}|/C$ in the spatial-temporal random HRM with $q = 2$. The red one denotes the position of the butterfly cone $\tau/w = q^2$.

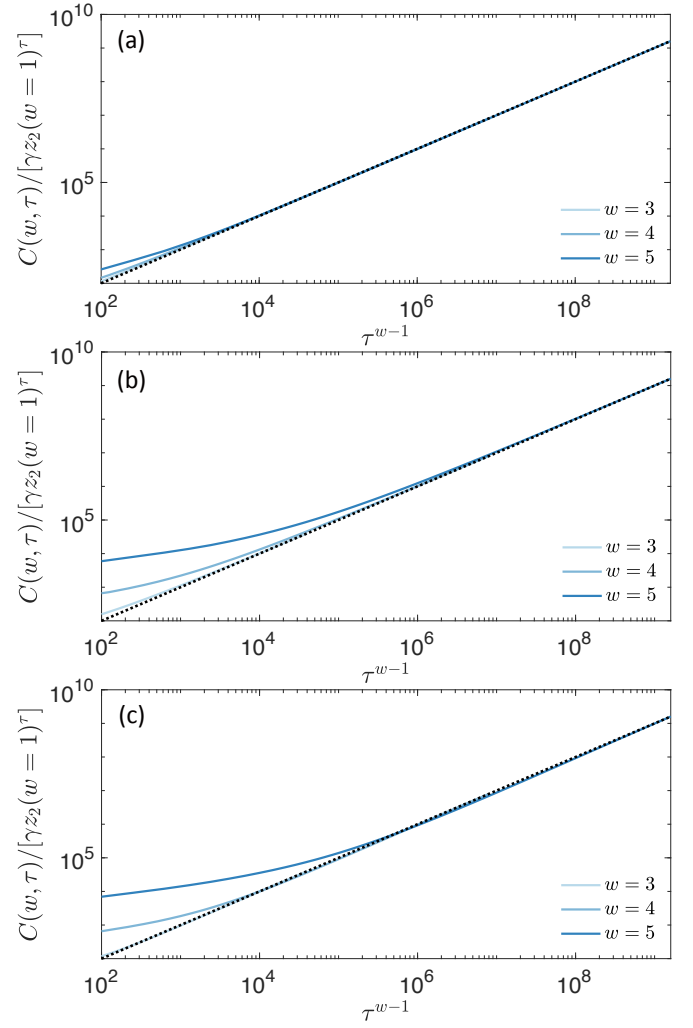


FIG. S13. Large τ behavior of the OTOC for (a) spatial-temporal random RPM, (b) spatial-temporal invariant 3PM, and (c) spatial-temporal invariant Z2-COE model. For the spatial-temporal invariant models, we use the same realization as that in the main text.

-
- [1] A. Nahum, J. Ruhman, S. Vijay, and J. Haah, *Phys. Rev. X* **7**, 031016 (2017).
 [2] J. c. v. Bensa and M. Žnidarič, *Phys. Rev. Res.* **4**, 013228 (2022).
 [3] A. Chan, A. De Luca, and J. T. Chalker, *Phys. Rev. Lett.* **121**, 060601 (2018).
 [4] B. Bertini, P. Kos, and T. Prosen, *SciPost Phys.* **8**, 67 (2020).
 [5] M. A. Rampp, R. Moessner, and P. W. Claeys, *Phys. Rev. Lett.* **130**, 130402 (2023).
 [6] P. Kos, B. Bertini, and T. Prosen, Correlations in perturbed dual-unitary circuits: Efficient path-integral formula (2020), [arXiv:2006.07304 \[cond-mat.stat-mech\]](https://arxiv.org/abs/2006.07304).
 [7] P. W. Claeys and A. Lamacraft, *Phys. Rev. Res.* **2**, 033032 (2020).
 [8] A. Nahum, S. Vijay, and J. Haah, *Phys. Rev. X* **8**, 021014 (2018).
 [9] C. W. von Keyserlingk, T. Rakovszky, F. Pollmann, and S. L. Sondhi, *Phys. Rev. X* **8**, 021013 (2018).